Czech University of Life Sciences Prague

Faculty of Agrobiology, Food and Natural Resources

Department of Water Resources

Saturated hydraulic conductivity measured on differently sized soil core samples

Diploma Thesis

Student: Batjargal Danaa

Supervisor: Prof. Ing. Svatopluk Matula, CSc.

2012

Declaration

I declare that I have elaborated my diploma thesis aimed at “Saturated hydraulic conductivity measured on differently sized soil core samples” independently and that I have used only the sources quoted in the “References”.

In Prague, 13 April 2012

Signature: …….

Contents

ACKNOWLEDGEMENT

First of all thanks a lot to my supervisor professor Svatopluk Matula who gave me the opportunity to perform this experimental work, especially in a newly constructed equipment and all his great support and guidance during whole project.

I wish to thank my consultant Markéta Miháliková and Kamila Báťková for the care and support, helping me with field and laboratory experiments and their valuable comments.

Special thanks to Ministry of Education, Youth and Sports of Czech Republic granted me a fellowship to study at Czech University of Life Sciences, Prague.

Special thanks to Mrs. Enkhtsetseg. D, MCS group and their financial support.

SUMMARY

This study is aiming at the estimation of different core sample size as parameter for soil physical properties and saturated hydraulic conductivity measurement. It concerns the manual reading of field experimental data collection quality at an experimental site of Czech University of Life Sciences in Prague equipped by a constant head infiltrometer.

A newly constructed constant head infiltrometer of the department design was used. It consists of two Mariotte's bottles system to reduce the measurement fluctuations caused by the disturbance created to water supply cut. The new equipment was tested firstly on a Chernozom type sandy loam soil in the field. And secondly the equipment tested in a laboratory on undisturbed soil samples from the same origin as the field experiment. Analytical and numerical data analysis methods were used to compare the influence of different size of soil core samples as well as manual and automatic reading technique.

Paying attention to the field saturated hydraulic conductivity, in-situ measurement techniques by infiltrometer accurate readings are considered, pointing out the main indications for the correct reading of each measuring approach. Laboratory automatic reading techniques are also considered.

Statistical data analysis showed that the results of saturated hydraulic conductivity performed by constant head infiltrometer which are measured on differently sized soil core (inner diameter of 5cm and 8cm) samples have no significant difference.

List of figures

List of tables

NOMENCLATURE

Symbol [dimension]	Description	Applied unit
A [L^2]	Cross sectional area	cm^2
d_i [L]	Inner diameter	cm
d_r [L]	Depth of insertion of the ring	cm
G	Shape factor	-
H [L]	Hydraulic head	cm
H_0 [L]	Initial hydraulic head	cm
H_1 [L]	Hydraulic head after water fall	cm
ΔH [L]	Hydraulic head difference	cm
h [L]	Steady state depth of ponded water	cm
i [LT^{-1}]	Infiltration rate	cm min^{-1}
i_c [LT^{-1}]	Characteristic infiltration rate	cm min^{-1}
I [L]	Cumulative infiltration	cm
I_h	Hydraulic gradient	-
K [LT^{-1}]	Hydraulic conductivity	cm min^{-1}
K(h) [LT^{-1}]	Unsaturated hydraulic conductivity	cm min^{-1}
K_s [LT^{-1}]	Saturated hydraulic conductivity	cm min^{-1}
K_{fs} [LT^{-1}]	Field-saturated hydraulic conductivity	cm min^{-1}
L [L]	Sampling ring height	cm

q [LT^{-1}]	Flow rate or flux	cm min^{-1}
r [L]	Ring radius	cm
T or t [T]	Time	min
v [LT^{-1}]	velocity	cm min^{-1}
Q [L^3T^{-1}]	Inflow or outflow	cm^3 min^{-1}
α	Significance level for statistical analysis	-
α [$M^{-1}LT^2$]	Shape parameter of the van Genuchten (1980) model	cm min^2 g^{-1}
Φ [L^2T^{-1}]	Matrix flux potential	cm^2 min^{-1}
μ [$M\ L^{-1}\ T^{-1}$]	Viscosity of water	g cm^{-1} min^{-1}
Ψ [L]	Soil water potential, water pressure head, tension	cm
$\Psi(\theta)$	Soil water retention curve	-
θ [L^3L^{-3}]	Volumetric water content	cm^3 cm^{-3}
θ_s [L^3L^{-3}]	Saturated water content	cm^3 cm
$\Delta\theta$ [L^3L^{-3}]	Difference between initial and saturated water content	cm^3 cm
ρ_b [ML^{-3}]	Soil bulk density	g cm^{-3}
ρ_s [ML^{-3}]	Soil particle density	g cm^{-3}
ρ_w [ML^{-3}]	Density of water	g cm^{-3}

1 INTRODUCTION

The saturated hydraulic conductivity is one of the most important soil hydraulic properties. The hydraulic conductivity is a quantitative measure of soil ability to transmit water. It defines the behavior of a soil water system to forced boundary conditions. When water moves through soil various forces act in response. It is very sensitive to soil porous media texture and structure. There are many different applications since it determined such as environmental protection, soil reclamation, irrigation and drainage for agricultural and non agricultural purposes, landfills, sport yard etc. It is also one of the primary input parameters for hydraulic models simulation.

A direct measurement of saturated hydraulic conductivity is always preferred in the all kind of studies. Klute, (1986) reported its importance. Many methods have been developed several years for field and laboratory measurements of saturated hydraulic conductivity. Unfortunately, these methods often yield substantially dissimilar results, as saturated hydraulic conductivity is extremely sensitive to sample size, flow geometry, and soil physical and hydraulic characteristics (Bagarello et al., 2000).

According to Bouma, (1983) most of the saturated hydraulic conductivity measurement methods are neither appropriate for all applications nor accurate for all soil types and conditions. The literature (Dunn and Philips, 1991) shows that regardless to the land practices a small portion of the soil volumes transports a large portion of the water flow, indicating that the spatial hydraulic characteristics of soils are highly variable. Saturated hydraulic conductivity measurements should therefore be evaluated carefully to ensure that the saturated hydraulic conductivity values obtained are accurate and appropriate for the intended use.

The most commonly used field methods to measure saturated hydraulic conductivity above water table are infiltration tests. The infiltration tests are determined by devices called usually infiltrometers. Commercially available ring or cylinder shaped infiltrometers are thin-walled, both ends are open, metal or plastic cylinders with an outside beveled cutting edge on the one end. Various types of cylinders are arranged including solitary cylinder and pressure infiltrometers.

In this study, a special newly constructed constant head infiltrometer, common soil core sampling rings of different sizes were used.

2 AIMS AND OBJECTIVES

There are three main objectives of the thesis:

The first objective of this study is to evaluate the influence of sampling technique and measurement technique in situ and comparing to the laboratory technique. And to identify factors which require more detailed investigations further.

The second objective of this study is to evaluate the effects of the hydraulic connections with the subsoil of the profile on the saturated hydraulic conductivity value and to include the influence of the core sample size and develop new techniques for the experiments.

The third one is to evaluate hypotheses of the assumptions.

Hypotheses are:

- The size of the soil sample ring has not significant influence on the measured saturated hydraulic conductivity in our soil.
- The subsoil hydraulic interaction supposes to have significant influence on the saturated hydraulic conductivity measurements in situ.

3 LITERATURE REVIEW

3.1 Review of measuring methods

When the soil media consists of two phases (water and soil particles) the flow of water is called Saturated flow. When the soil porous media consists of three phases (water, soil particle and air) system it is called Unsaturated flow. The main difference between unsaturated and saturated flows distinguishes in the hydraulic conductivity. When the soil is saturated, all pores are filled with water. When the soil is unsaturated some of the pores entrap air so that the conductive portion of the soils cross sectional area is diminished. Unsaturated hydraulic conductivity determination is more difficult to compare the saturated hydraulic conductivity determinations. Several methods exist for lab determination of unsaturated hydraulic conductivity such as Steady state method (Klute and Dirksen, 1986), Outflow method (Gardner, 1956), Hot wind method (Arya et al, 1975), Centrifugal method (Conca and Wright, 1992) etc. Field method example is Tension infiltrometer (Perroux and White, 1988) for unsaturated flow.

The saturated hydraulic conductivity K_s can be measured in a laboratory or in a field. Direct laboratory methods are constant or falling head permeameters (Klute and Dirksen, 1986). In situ, if the ground water table is close to the soil surface and K_s measurements below the water level Auger-hole method or Piezometer methods are the most common ones. If ground water table is deep, above water level measurements such as single or double-ring infiltrometer tests (Bouwer, 1986), the pressure infiltrometer, tension disc infiltrometer, mini disc infiltrometer and the Guelph permeameter (Reynolds and Elrick, 2002) can be used to determine K_s.

Several methods exist to measure the saturated hydraulic conductivity in both the unsaturated and saturated zone (Baetens, 2007). Methods for the latter condition will not be discussed because they are not important for this thesis. K_s field methods for the unsaturated zone can be subdivided into two main categories such as the ring infiltrometers (Reynolds et al., 2002) and the constant head permeameters (Reynolds and Elrick, 2002).

Single and double-ring infiltrometers, pressure infiltrometers and multiple ring infiltrometers belong to the ring infiltrometers. The single and double-ring infiltrometers are typically metal cylinders which are driven into the soil and then steady-state infiltration rates are determined

applying falling or constant head techniques. A method to analyze infiltration data from a single-ring infiltrometer will be outlined further. A double-ring infiltrometer consists of a single ring around which a second larger ring is placed and driven into the soil. Water is ponded between the two rings in order to reduce edge effects and to maintain vertical flow below the central cylinder (Reynolds et al., 2002). Many designs of pressure infiltrometers has been developed until now. (Example: Matula and Kozáková, 1997)

The Guelph permeameter belongs to the category of the constant head permeameters. The permeameter is a down-hole Mariotte devive and maintain the level of water in the hole in the soil consistently. And the infiltrated water volume is to be measured easily. By measuring the steady-state infiltration rate at different ponded height it is then possible to calculate the field-saturated hydraulic conductivity (Reynolds et al., 1983).

3.1.1 Field methods

Conventional field methods to measure saturated hydraulic conductivity are the Auger-hole method, piezometer or single and double ring infiltrometers. Single and double ring infiltrometers can only measure water flow under ponded (saturated) conditions.

Auger-hole method:

The general principle of Auger-hole method is simple. A hole is bored into the soil to a certain depth below the water table. When equilibrium state is reached with the surrounding ground water, some amount of the water in the hole is lowered by pumping or bailing. The water seeps into the hole again, and the rate at which the water rises in the hole is measured and then converted by a suitable formula to the hydraulic conductivity of the soil.

The Auger-hole method gives the average permeability of the soil layer extending from the water table to a small distance below the bottom of the hole. This method is appropriate for single layered soil. If there is an impermeable layer at the bottom of the hole, the value of K_s is governed by the soil layers above this impermeable layer. The use of this method is limited to areas with a high ground water table.

Double ring infiltrometer:

The double ring infiltrometer consists of an inner and outer ring. Both rings inserted into the ground and each ring is supplied with a constant head of water. The outer ring helps in reducing the error that may result from lateral flow in the soil. The rate of infiltration is measured by amount of water, known surface area due to the parameters of the inner ring, infiltrates per unit of time. Hydraulic conductivity can be estimated for the soil when the water flow rate in the inner ring is at a steady state. (http://www.usyd.edu.au/agric/web04/double%20ring)

Some draw-backs of the double ring are that it is very time consuming, requiring frequent attention, either by recording measurements or by maintaining equilibrium in the height between the rings. The rings are heavy to transfer. It also requires a flat undisturbed surface which sometimes is not available. The infiltration rate varies with different soil types, which can effect the accuracy of the results. (McKenzie et al., 2002). Results from this double ring infiltrometer

can be taken only as directory information. However they can be considered as accurate enough for some applications e.g. design of the sport surface, land drainage pipes, landfill isolation layers, etc.

When use above methods in soil with distinct macropores, preferential flow will dominate. This does not take place under processes like rain or conventional irrigation system. Therefore many authors attempted to create a negative potential (tension) on the water flow.

Angulo-Jaramillo et al., (2000) divided infiltrometers into two groups:

a. Tension disc infiltrometers
b. Pressure ring infiltrometers

According to Philip, (1969); Reynolds and Elrick et al., (1990) both the pressure and tension infiltrometer methods allow to establish of a three-dimensional infiltration process that accomplishes steady-state conditions after a transient phase.

a. Tension disc infiltrometer

Gardners, (1939) developed a negative head permeameter. Dixon, (1975) developed a closed-top ring infiltrometer to quantify macropores. Water is applied to a closed-top system, which permits the imposition of negative pressure on the ponded water surface. Negative tension can be considered as simulating a positive soil air pressure, created by a negative air pressure above ponded surface water. A simplification was made by Topp and Zebchuk, (1985). The limitation of this device is the infiltration which has to be started by ponding (positive head) the closed-top infiltrometer, then adjusted to a negative pressure. (http://en.wikipedia.org/wiki/disc_permea)

Some research effort was continued in this, instead attention has been given mainly to the sorptivity* apparatus of Dirksen, (1975) which used a ceramic plate as a base. Based on his design, Clothier and White, (1981) developed the sorptivity tube which can provide a constant negative potential (tension) on the soil surface. However, the sorptivity tube had some shortcomings, hence modifications to the design led to the development of the disc permeameter by Perroux and White, (1988). It is also known as the tension infiltrometer.

* Sorptivity as a measure of the porous medium to absorb or desorb liquid by capillary action (Philip, 1957)

The tension infiltrometer methods can be divided into three groups: single disk with single tension; single tension with discs having different radii; and single disk with multiple tensions (Reynolds et al., 2000). Single tension with discs having different radii: The hydraulic conductivity is calculated from the infiltration rates of two, or three experiments employing discs of different radii only for one tension. Smettem and Clothier, (1989) modified the twin ring method of Scotter et al., (1982) by extending the ponded method to unsaturated discs of two contrasting radii. Thony et al., (1991) developed an alternative approach which is based on using three discs of different radii. Single disc with multiple tensions: This method is more advantageous, because only one infiltrometer (disc) is needed to determine the unsaturated hydraulic conductivity. Perroux and White, (1988) presented designs for tension infiltrometers, where water could be supplied at both positive and negative tensions (Figure 1a and 1b). Angulo-Jaramillo, (2000) following the design of Perroux and White, (1988) developed a system of three tension infiltrometers TRIMS - triple ring infiltrometers at multiple suction to evaluate and compare multiple disc approach with a single disc at multiple tensions approach.

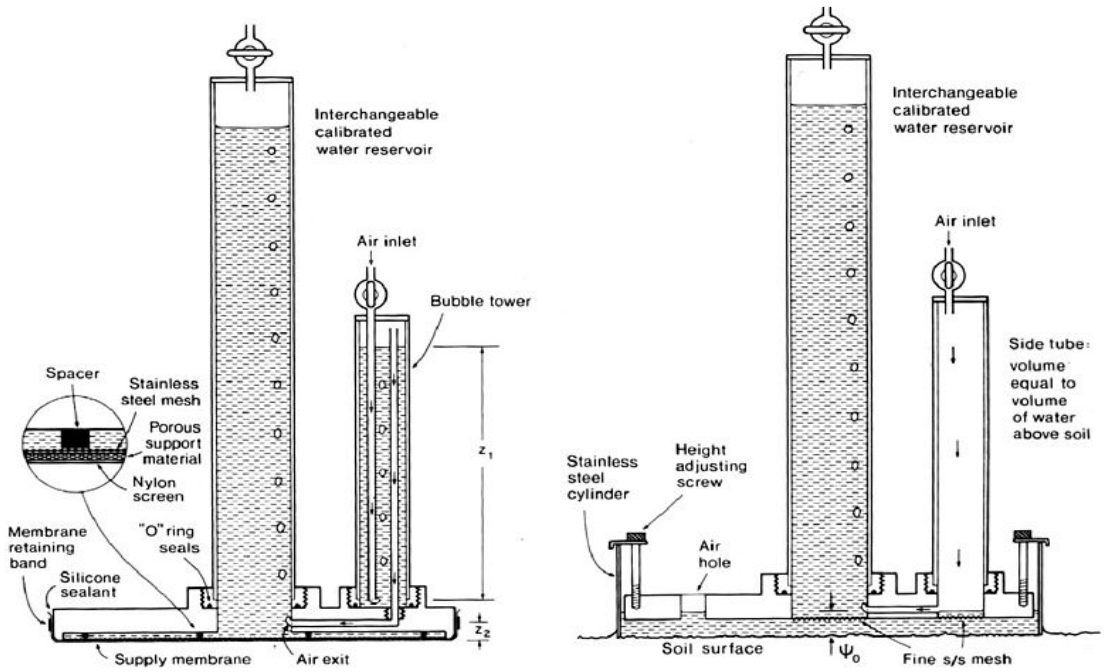

a. b.

Figure 1. Infiltrometer diagram. a. at negative pressure, tension; b. at ponded, positive pressure (http://en.wikipedia.org/wiki/Disc_permeameter)

b. Pressure infiltrometers

The pressure infiltrometer is designed to measure K_s at the soil surface, with minimal disturbance of it. A sealed ring is driven a known depth into the soil, after which a constant head is applied until near steady-state infiltration rate is reached (Reynolds and Elrick, 1991).

Pressure infiltrometers are used mainly to measure saturated hydraulic conductivity, but can also be used to determine matrix flux potential, sorptivity, macroscopic capillary length parameter, the effective wetting front, pressure head, air entry pressure head and water entry pressure head. The method is based on ponded infiltration through ring inserted certain depth into unsaturated soil.

A relatively simple pressure infiltrometer (Matula and Kozáková, 1997) is a Mariotte type infiltrometer (Figure 2) consists of non corrosive materials (plastic cylinder, Teflon and PVC). The device principally works according to mechanical hydraulic force. It doesn't require any external energy source. It is a portable device, simple to operate and set up. The device enables to measure ponded cumulative infiltration from a small diameter of infiltration ring with satisfactory accuracy.

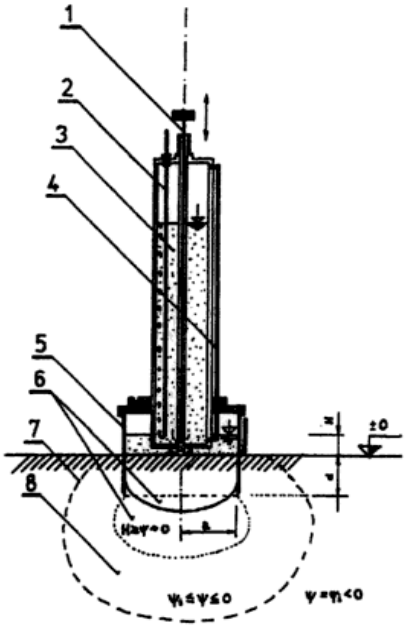

1- Piston valve to open/close the water outlet
2- Moveable air tube to set the applied water pressure *H* on infiltrating surface
3- Mariotte type water reservoir
4- Plexiglass tube of a small diameter to enable accurate reading of the corresponding water level
5- Infiltrometer ring
6- Bulb of field saturated soil
7- Wetting front

Figure 2. Schematic diagram of pressure infiltrometer. (Matula and Kozáková, 1997)

The major components of the ponded infiltrometer are a Mariotte's bottle, a valved base and a containment ring. Mariotte's bottle is a cylindrical shaped bottle or tank which delivers a constant rate of flow from closed system. It is named after French physicist Edme Mariotte (1620-1684). The design of Mariotte's bottle with stopper and air inlet via siphon was again reported by McCarthy (1934). The pressure at the bottom of the air inlet tube is always the same as the pressure outside the reservoir. Thus air can be in. If the entrance to the siphon is at the same depth, then it always supplies the water at atmospheric pressure and delivers a flow under constant head height, which refers to the water level drop in the Mariotte's bottle.

This principal has many variations in apparatus design and it has been used widely when a constant water pressure is required, supplying water at constant head and measuring infiltration rate in soil. The drawback of the design is that it is sensitive for gas inlet leakage and that during operation liquid cannot be added, since it would change the pressure control. Nowadays accurate control is supported by electronic devices.

3.1.2 Laboratory methods

Hydraulic conductivity in saturated zone can be measured with two types of laboratory apparatuses: constant head permeameter and falling head permeameter. Undisturbed soil samples are typically used to measure K_s. But in case if disturbed samples are tested in such permeameters, it is important to note that they should be carefully saturated with water by the aid of an upward flow through the soil column. During the development of the experiment, the certain water head has to be maintained.

a. Constant head apparatus

The constant-head method (Figure 3) is typically used on granular soil which its saturated hydraulic conductivity is higher than fine grained soil. This procedure allows water to move through the soil under a steady state head condition while the quantity of water flowing through the soil sample is measured over a period of time.

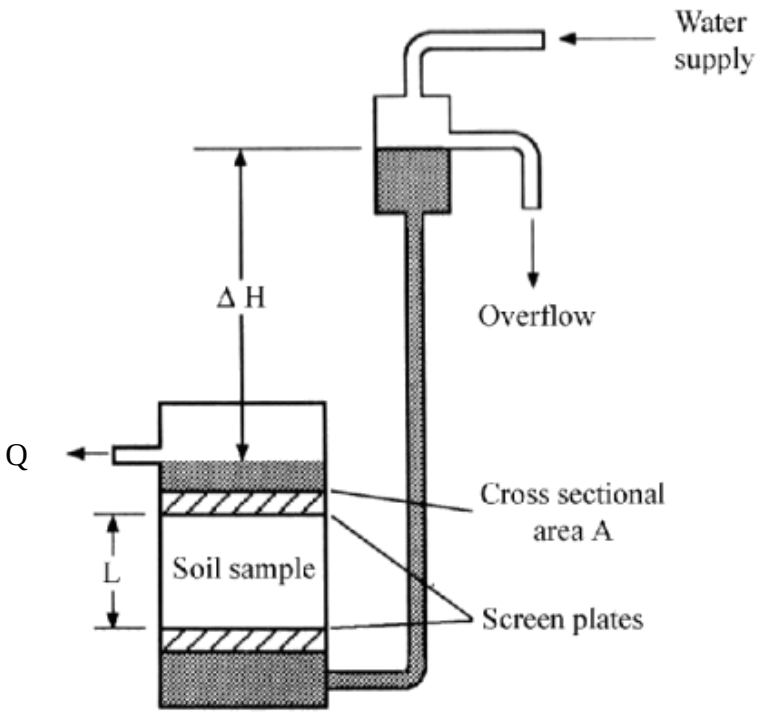

Figure 3. Constant head apparatus (http://echo2.epfl.ch/VICAIRE/mod_3/chapt_8/main.htm)

In this case, Darcy's law is applied to a soil sample of length L and a cross sectional area A through which a constant flow rate Q is generated by a constant head differential (Equation 1). By knowing the quantity Q of water flow measured, length L of sample, cross-sectional area A of soil sample, time t required for the quantity of water Q to be discharged, and hydraulic head ΔH, the saturated hydraulic conductivity can be calculated using Darcy's law (Equation 2):

$$Q = Av \tag{1}$$

where v is the flow velocity, [L T^{-1}]

$$v = KI_h \tag{2}$$

and expressing the hydraulic gradient I_h as:

$$I_h = \frac{\Delta H}{L} \tag{3}$$

where ΔH [L] is the difference of hydraulic head over distance L [L].

$$Q = -A \cdot K \cdot \frac{\Delta H}{L} \tag{4}$$

Solving K [L T^{-1}]:

$$K = -\frac{Q \cdot L}{A \cdot \Delta H} \tag{5}$$

Before starting the measurement, the sample should be completely saturated because the air bubbles will reduce the cross sectional area and lower the hydraulic conductivity. The preferential pathways along the wall of the column have to be avoided.

b. Falling head apparatus

The falling-head method is totally different than the constant head methods in its initial setup. However, the advantage to the falling-head method is that it can be used for both fine-grained and coarse-grained soils.

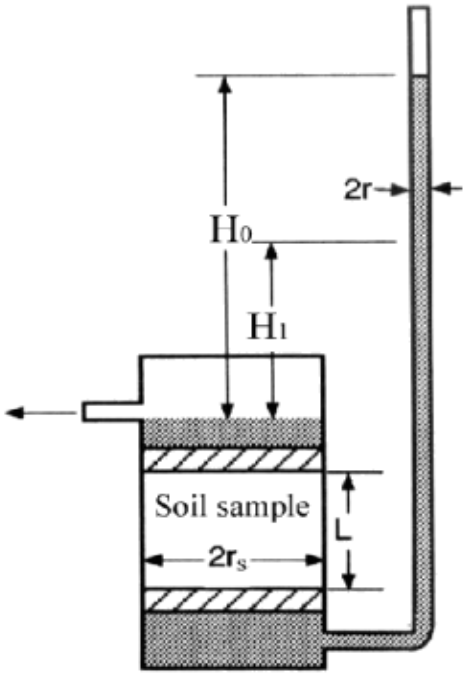

Figure 4. Falling head apparatus (http://echo2.epfl.ch/VICAIRE/mod_3/chapt_8/main.htm)

The soil sample is first capillary saturated then water allowed to flow through the soil without maintaining a constant pressure head. The falling head permeameter (Figure 4) is used for cohesive sediments, with low hydraulic conductivity. The time *t* during which the head in a tube of radius *r*, attached to the permeameter and supplying the sample, falls from H_0 to H_1 is measured with such a permeameter. The following relationship gives the resulted flow rate:

$$Q=\pi r^2 \cdot \frac{dh}{dt} \qquad (6)$$

In this case, for the sample with a cross sectional area *A* and with the length *L*, Darcy's law (Equation 4) can be followed.

Solving the equations 4 and 6 will be obtained:

$$\pi r^2 \cdot \frac{dh}{dt} = \mathrm{A} \cdot \mathrm{K} \cdot \frac{h}{L} \qquad (7)$$

The column of soil sample is considered to have a cylindrical shape, described by a radius r_s. The result after integration should be:

$$\mathrm{K} = \frac{r^2 \mathrm{L}}{{r_s}^2 \mathrm{t}} \ln\left(\frac{\mathrm{H_o}}{\mathrm{H_1}}\right) \qquad (8)$$

3.1.3 Other estimation methods

Several models have been developed for describing the soil water retention curve and saturated hydraulic conductivity based on discrete measurements. Although many techniques are available, most of them remain time consuming and costly, and consequently many researchers have searched for and found alternative methods to estimate these properties. Pedotransfer function (PTFs) is a good example of this solution. (Baetens, 2007)

In general some analytical models can be fit to experimental data. When, no experimental data are available or obtainable pedotransfer functions (PTFs) can be used to estimate either the soil hydraulic parameters used in analytical models such as the van Genuchten (1980) model or a discrete set of data pairs of the soil water retention $\psi(\theta)$ curve.

Such PTFs have been obtained by regression techniques, artificial neural networks, classification and regression trees (CART), group method of data handling (GMDH) and fractal mathematics (Wosten et al., 2001). Independent from the technique used, there exists a lot of uncertainty in applying PTFs to soil conditions different from those under which PTFs were derived (e.g. stone content) (Cornelis et al., 2001; Lee, 2005). For that reason PTFs have to be used with caution.

3.2 Review of affecting factors for saturated hydraulic conductivity determination

Saturated hydraulic conductivity is affected by both soil and testing fluid properties. It depends on the soil pore geometry as well as the viscosity and density of fluid. The hydraulic conductivity for a given soil becomes lower when the fluid is more viscous than water. Pore geometry and continuity within a soil or landscape vary depending on the direction of measurement. The vertical component of K_s can be different from the horizontal component.

It is important to preserve the texture-structure interaction is that the antecedent structure by both the core/ column collection procedure and K_s measuring technique in order to measured K_s value to be a representative of the porous medium in its natural condition (Reynolds et al., 2002). Following factors should be considered for saturated hydraulic conductivity determination:

1. Soil layer texture (particle size distribution, porosity). Soil textural–structural conditions are critically important factors determining both the magnitude of saturated hydraulic conductivity and the best methods for measuring it. The K_s value tends to increase greatly with coarse texture because of an increase in the number and size of large, high water conductive pores. (Dane and Topp ed. 2002)
2. Soil structure (cracks, worm holes, plant root channels). Also rock fragments can have a profound impact on measured hydraulic properties of which the spatial variation influences the amount and distribution of infiltration, and as a consequence the amount of overland flow. Rock fragments present in soil influence soil hydraulic properties by affecting soil porosity and water flow paths (Baetans, 2007). As rock fragment content increases, the area available for water flow decreases, and overall water movement can become restricted. But increasing rock fragment content the creation of new voids in the stone-earth contact can increase the saturated hydraulic conductivity.
3. Seasonal affects and time trend. Just above the freezing temperature of water is useful to inhibit microbiological activity and soil structure influence. (Klute, 1986). Microorganisms are naturally occurring part of the soil. Therefore development of microorganisms can not be suppressed.

4. Soil salinity and acidity (Sodium ion decreases hydraulic conductivity, while Magnesium ion increases it). The dissolved salt ions and their concentrations in the water can affect K_s through flocculation or dispersion of clay part within the porous medium. Flocculation of clay will cause K_s to increase by increasing the size and numbers of water transmitting pores. Dispersion of clay will decrease K_s by blocking pores with clay particle. Extensive clay dispersion will reduce the K_s of a soil to virtually zero (Dane and Topp, ed. 2002). Water used for measuring the K_s of a natural porous medium should be therefore either native water extracted from the porous medium, or a laboratory approximation that has the same major ion speciation and concentrations as the native water. Local municipal tap water is often an adequate approximation to the native water. Although this should always be checked. Distilled or deionized water shouldn't be used for measuring the K_s of a natural porous medium, as these types of water encourage clay dispersion (Reynolds and Elrick et al., 2002).
5. Microbiological activity is very important time dependant affect on K_s, usually decreases K_s (Reynolds and Elrick et al., 2002). Earthworms and ants can increase the macrostructure of the soil through time, and can even open up macro pores extending the entire length of the core which cause pipe flow of water may subsequently occur. But the growth of algae within the soil sample and on the soil surface, in other hand, can gradually block soil pores, and therefore cause a time dependent decrease in the measured K_s value. Earthworm burrowing can be stopped storing the soil cores for a period of time (5 – 7days) at temperature that is sufficiently below freezing to kill the earthworms is about -5°C (Reynolds and Elrick et al., 2002)
6. Geomorphology – Swelling clay minerals change chemical composition of soil. So large effect on K_s. Oosterbaan and Nijland, (1994) reported the coarser soil particles (sand and silt) are deposited near the river banks, whereas the finer particles (silt and clay) are deposited in the back swamps further away from the river. The coarse soils usually have a fairly high K_s. This factor is not important for this study. Therefore it will not be considered.

7. Testing liquid properties. Freshly tapped water is improper for measurement. It reduces K_s. It has tremendous air in. Also hydraulic conductivity is directly proportional to testing water viscosity, and water viscosity is inversely proportional to temperature. For example: an increase in water temperature from 10 to 25°C will result in a 45% increase in K_s all other factors remaining constant. Precise measurements and comparisons of K_s values should be therefore always be corrected to a reference water temperature. (Reynolds and Elrick et al., 2000).
8. Entrapment of air. Bubbles of air entrapped within the porous medium physically block pores and can thereby cause the K_s to be less than when the material is completely saturated. In relatively structureless materials, entrapped air can reduce the measured K_s by a factor of two or more. (Bouwer, 1978) Air bubbles occur through entrapment of resident air by the infiltrating water when the porous medium is being wetted up, and through exsolution of air that was initially dissolved in the infiltrating water. Air entrapment and exsolution problems are minimized (but not necessarily eliminated) by slow bottom up wetting of porous medium under vacuum using water that has been de aired by boiling, autoclaving or aspiration into a vacuum (Klute, 1986). The saturation process might be also enhanced by replacing the air in the pores with carbon dioxide before starting the saturation process. As carbon dioxide is highly water soluble, any bubbles entrapped during the saturation process will dissolve quickly into the infiltrating water (Reynolds et al., 2002)
9. Core sample size. Many soil properties show great spatial variation. This variability is the result of intrinsic (natural) or extrinsic (cultural or management related) processes. Furthermore, it has to be taken into account that soil properties do not refer to a point in the soil system, but to a certain macroscopic volume. Sampling a very small volume results in a extreme variation in the measured soil properties, sampling sequentially larger soil volumes reduces the range of results until a large enough volume is reached and each measurement gives the same result (McBratney, 1998). The sample volume at which this occurs, is the elementary representative volume (REV) (Figure 5).

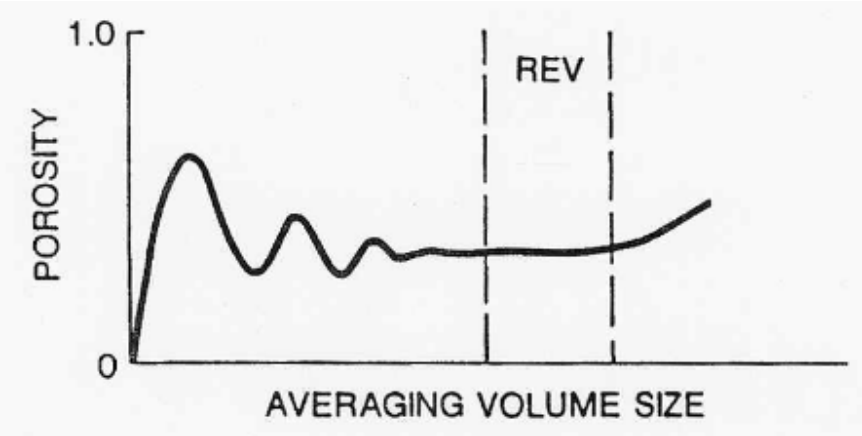

Figure 5. The representative elementary volume concept (after Bear 1972)

The range of sample volumes over which a given variable is invariant has been defined as the REV-domain. Buchter et al., (1994) demonstrated this principle clearly for the coarse fragment content of a Swiss soil which decreased exponentially to an asymptomatic value with increasing sample volume. They estimated the representative elementary volume for determination of the coarse fragment content between 0.4 10^{-3} m^3 and 2.1 10^{-3} m^3. In laboratory, the size of the REV should be theoretically estimated in order that an appropriate soil core sampler should be selected. In practice, REV is rarely determined. Therefore standard core or metal cylinders are used. K_s is extremely sensitive to even small differences in sample size, flow geometry and soil structure (Bouma, 1983)
Standard core is a soil sampling ring. It is also known as Kopecky ring.

3.3 Review of data analysis methods

In general, saturated hydraulic conductivity is calculated from Darcy's law based on measuring soil water flux and hydraulic gradient. The three-dimensional steady-state flow in saturated soils can be described using the law of Darcy:

$$q = -K_s \cdot \left[\frac{\partial H_x}{\partial x} ; \frac{\partial H_y}{\partial y} ; \frac{\partial H_z}{\partial z}\right] \quad (9)$$

where $H_{x, y, z}$ [L] is the hydraulic head and K_s [L T^{-1}] is the saturated hydraulic conductivity defined as the discharge observed per unit area at a unit hydraulic gradient and mainly depending on soil structure and particle size (Reynolds et al., 2002).

Many authors (Reynolds and Elrick, 1990; Wu and Pan, 1997) presented and discussed steady state theory.

- There are many models and system to describe saturated hydraulic conductivity, but the reliability of these depends on how accurate we can achieve the different assumptions which were created.
- The interpretation of our final results always must be considered the model's assumptions.
- The spatial variability of K_s in a soil is too high, so sometimes when we want to represent a soil with a unique value is useful to do a statistical analysis in order to find to the most representative value of K_s.
- The representative K_s value is defined for the specific purpose, for which will be used.

Because of entrapped air during the infiltration process, field saturated hydraulic conductivity could be lower than hydraulic conductivity in completely saturated conditions. Thereby, K_s will be referred to respectively for infiltrometer test.

Single ring pressure infiltrometer measurements:

According to steady-flow conditions, flow rate of a ring infiltrometer is given by:

$$Q = \left(\pi r^2 + \left(\frac{r}{G}\right)\left(H + \frac{1}{\alpha}\right)\right) K_s \qquad (10)$$

where Q [$L^3\ T^{-1}$] is steady state infiltration rate, r[L] is radius of the ring, H[L] is the steady value of hydraulic head applied during the measurement α[L^{-1}] is a parameter, K_s[$L\ T^{-1}$] is the saturated hydraulic conductivity, G[$L^3\ T^{-1}$] is a shape parameter given by:

$$G = 0{,}316\frac{d_r}{r} + 0{,}184 \qquad (11)$$

and r[L] is the ring radius, d_r is the depth of insertion of the ring into the soil (Reynolds and Elrick, 1990).

The accuracy of measurements by single ring pressure infiltrometer can be affected by other factors: during the insertion of the infiltrometer ring, soil macrostructure can collapse for soil matrix compression (or soil shattering), and the wall of the ring can cut off non-vertical pores.

Reynolds and Elrick (1990) developed a method to calculate saturated hydraulic conductivity from obtained data. According to their method the field-saturated hydraulic conductivity K_{fs} follows from:

$$K_{fs} = \frac{q_s}{\pi \cdot R_s^2\left(\frac{H}{C_1 d + C_2 R_s} + \frac{1}{[C_1 d + C_2 R_s]} + 1\right)} \qquad (12)$$

where q_s [$L^3\ T^{-1}$] is the steady-state flow rate, R_s [L] is the ring radius, H [L] is the steady-state depth of ponded water in the ring and d [L] is depth of ring insertion into the soil. The coefficients C_1 = 0.316 and C_2 = 0.184 are dimensionless quasi-empirical constants that apply for d ≥ 3cm and H ≥ 5cm.

One of the major drawbacks limiting the use of Equation (12) are the boundary conditions that have to be met, otherwise the coefficients C_1 and C_2 depend on the depth of ring insertion and the height of ponded water in the ring.

A more generalized solution to describe infiltration from single-ring infiltrometer was developed by Wu and Pan (1997) using scaling techniques. Their infiltration equation can be written as:

$$\frac{i}{i_c} = a + b\left(\frac{t}{T_c}\right)^{-0.5} \quad (13)$$

where i [L T^{-1}] is the infiltration rate, i_c [L T^{-1}] is the characteristic infiltration rate, t [T] is the time, T_c [T] is the characteristic time scale, a and b are dimensionless constants (a = 0.9084, b = 0.1682).

When one measures the cumulative infiltration I [L], parameter B can be calculated by equation (14) (Philip, 1957):

$$I = Bt + C\sqrt{t} \quad (14)$$

where: B and C are parameters related to hydraulic conductivity and sorptivity.

The hydraulic conductivity of the soil K is calculated as follows:

$$K = \frac{B}{A} \quad (15)$$

where A is van Genuchten parameter relating the soil texture classes.

Wu and Pan (1999) found the K_s-values determined using their method to be comparable with those calculated using the single head method of Reynolds and Elrick (1990) and close to the true values determined for three different types of soils using numerical tests.

Unsaturated flow is more complicated and based on proper assumptions and conditions, governing equation (16) is called Richard's equation:

$$\frac{\partial\theta}{\partial t} = \frac{\partial}{\partial z}\left[K(h)\left(\frac{\partial \mathrm{H}}{\partial z} + 1\right)\right] \quad (16)$$

where K(h) is unsatuated hydraulic conductivity [L T^{-1}], H is the pressure head [L], z is elevation head [L], θ is the water content [L^3 L^{-3}], t is time [T].

Richard's equation is valid in terms of hydraulic head:

$h=H+z.$ (17)

Relationship of unsaturated and saturated hydraulic conductivity estimation equations (equation (18) Gardner, 1958, equation (19) Gardner and Mayhugh, 1958, equation (20) Brooks and Corey, 1964) are:

$K(h) = K_s \exp(ch)$ (18)

$K(h)= K_s \exp(c(h-h_v))$ (19)

$K(h)/ K_s = (h_v/h)^m$ (20)

where: K(h) is unsaturated hydraulic conductivity[$L\ T^{-1}$], K_s – saturated hydraulic conductivity [$L\ T^{-1}$], h is soil water potential [L].

c -empirical constant, depending on particle size distribution, ($c=0.1\text{-}0.01 cm^{-1}$)
h_v – air entry value
m-coefficient related to the pore distribution

4 MATERIALS AND METHODS

Factors affecting the determination of the saturated hydraulic conductivity on the samples of different size and with the connection to the subsoil layers and without this connection evaluated on the basis of the laboratory and field experiments.

Two different sizes of sampling rings made from metal were used. Their dimensional characteristics are below:
"Small ring" - its inner diameter is 5.0cm. Height of the ring is 5.1cm. Volume is 100cm³.
"Big ring" - inner diameter is 8.0cm. Height is 5.0cm. Volume of the big ring is 251cm³. Both of them were not yet a representative elementary volume (REV).

To maintain a certain ponded water head on sampling ring surface sticky plastic tape (height of the tape is 2.0cm) has been used. The plastic tape was not easy solution to keep exactly the same height for all replicate measurement.

The ponded head infiltration measurements were done using a newly constructed constant head infiltrometer. It is described further in field experiment. In brief, the pressure infiltrometer consists of 2 Mariotte type cylinder bottles (height 49cm, weight 1154g), rubber stoppers with air entry and refilling tubes, teflon valves, connectors and Plexiglas tubes. The total height of the infiltrometer is 53.5cm including base and stopper, volume is 2000cm³, each cylinder reservoir inner diameter of 10.5cm, height of 44cm and the total weight when filled with water is 3154g.

Total tare weight of the new equipment is 2354g. Total weight filled with water is 6354g.

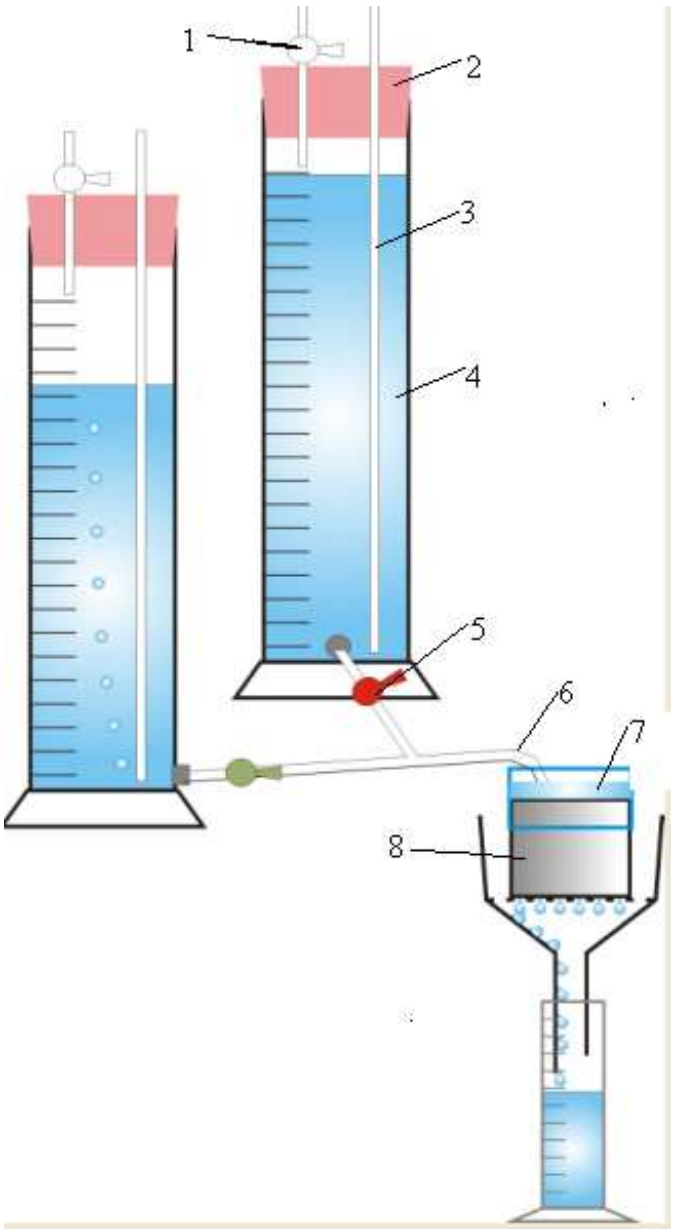

1 – Refilling tube and valve
2 – Rubber stopper
3 – Bubbling tube, to set the water pressure on infiltrating surface
4 – Mariotte type cylinder reservoir
5 – Teflon valve open/close water inlet
6 – Plexiglass tube
7 – Constant water head on soil surface
8 – Soil core sample

Figure 6. Schematic diagram of new equipment

A valve is on top of the rubber stopper and the water reservoir to enable refilling with no any disturbance to the infiltration surface. The infiltrometer does not need to be removed from the surface. This was the big advantage of this construction with two water reservoirs and easy switching, thus the water can be refilled during the experiment.

The infiltration experiments can be illustrated as shown Figure 7 .

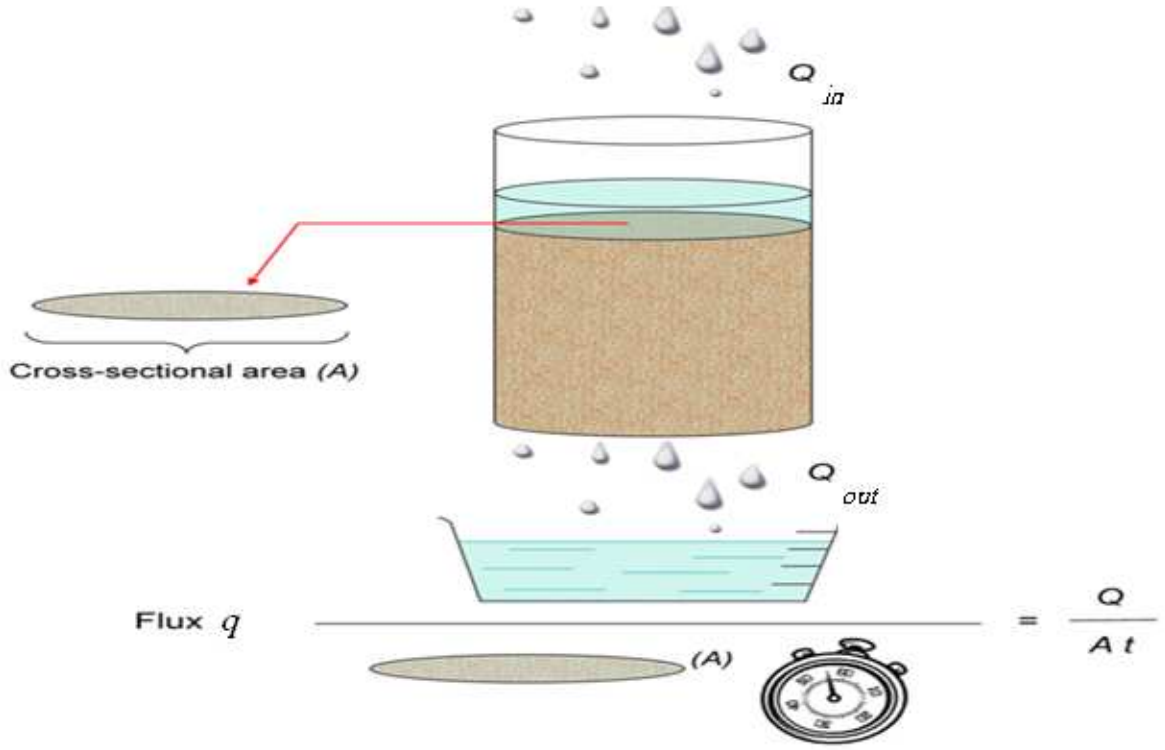

Figure 7. Illustration of infiltration process (Soil survey technical note 6, USDA, NRC, 2004)

The both experiments field and lab followed by Constant head technique and equation (4 and 5) can be rewritten as equation (21):

$K_s = Q\ L / A\ \Delta H\ t$ (21)

where:

Q – inflow of water, cm^3

L – soil sample length, cm. For this study it equals the insertion depth of infiltrometer ring. Which is for big ring L=5cm, for small ring L=5.1cm.

A – cross sectional area, cm^2. $A=\pi r^2$ for cylindrical shaped sample

ΔH – inflow and outflow difference, cm

t- time, min

4.1 Field experiment

The in-situ infiltration tests took place between the 16 November and 20 November 2011 in the experimental field of Czech University of Life Sciences on a sandy loam (according to soil type it is Chernozem) soil the same that used for the laboratory experiments. Vegetation was permanent grass. Field condition example is in Table 1.

Table 1. Field experiment condition (one day example)

Location: CULS potato field		Big ring No:	6
Date: 20 Nov 2011	Weather: Mostly cloudy	θ initial:	Note:
Tillage treatment: Permanent grass	Temp: +4 °C	26.0%	L=5.0cm r=4.0cm h=1.5cm
Sign. Rep 14 (Set 2)	Const. level height: 1.5cm		

Prior to all measurements, 16 measurement plots divided into two different sets (Figure 8) were chosen. Criteria used for the selection of representative plots were the soil compaction, observing the grass dense and tractor path. A tractor pathway shouldn't be included in order to avoid influence of soil compaction on the measurement. However it was not a hundred percent sure that there was no influence of soil compaction. The soil also can be affected of people walking or driving tractor. The weather conditions during the experimental period were cold and relatively dry. Day time temperatures ranged between -1°C - +5°C during the experiment period (no precipitation).

The measurements were conducted using a constant head infiltrometer. The soil surface was smoothened and leveled, the layer with grass root was removed approximately 5.0cm before the infiltrometer rings were placed onto the plots. The sandy loam soil was relatively easy to smoothen and level it using a knife. The rings, made of metal, had inner-diameters d_i of 5.0cm for small, 8.0cm for big ring and height of 5.0cm big ring and 5.1cm small ring. The rings were hammered down into the soil until full depth of the ring into the ground. Then the grass residue was clipped and leaf litter was removed from the soil surface by tearing scissors. The measuring

devices were placed on the surface straight away, because the surface was perfectly smoothened and leveled.

The one set of replicates were placed approximately 10cm to 30cm apart from each others. The distance between two sets was 1.5m. A constant ponded head, for which a value of 1.3cm to 1.6cm (supported plastic tape) was maintained by the Mariotte's bottle system of cylinder reservoirs. The target setting was 1.5cm. Each replicate constant water head was measured individually. After filling the ring carefully with water until it reached a water level slightly higher than 1.5cm, the infiltrometer was set to the appropriate head and the actual readings were initiated from the moment the first air bubbles developed in the Mariotte's bottle.

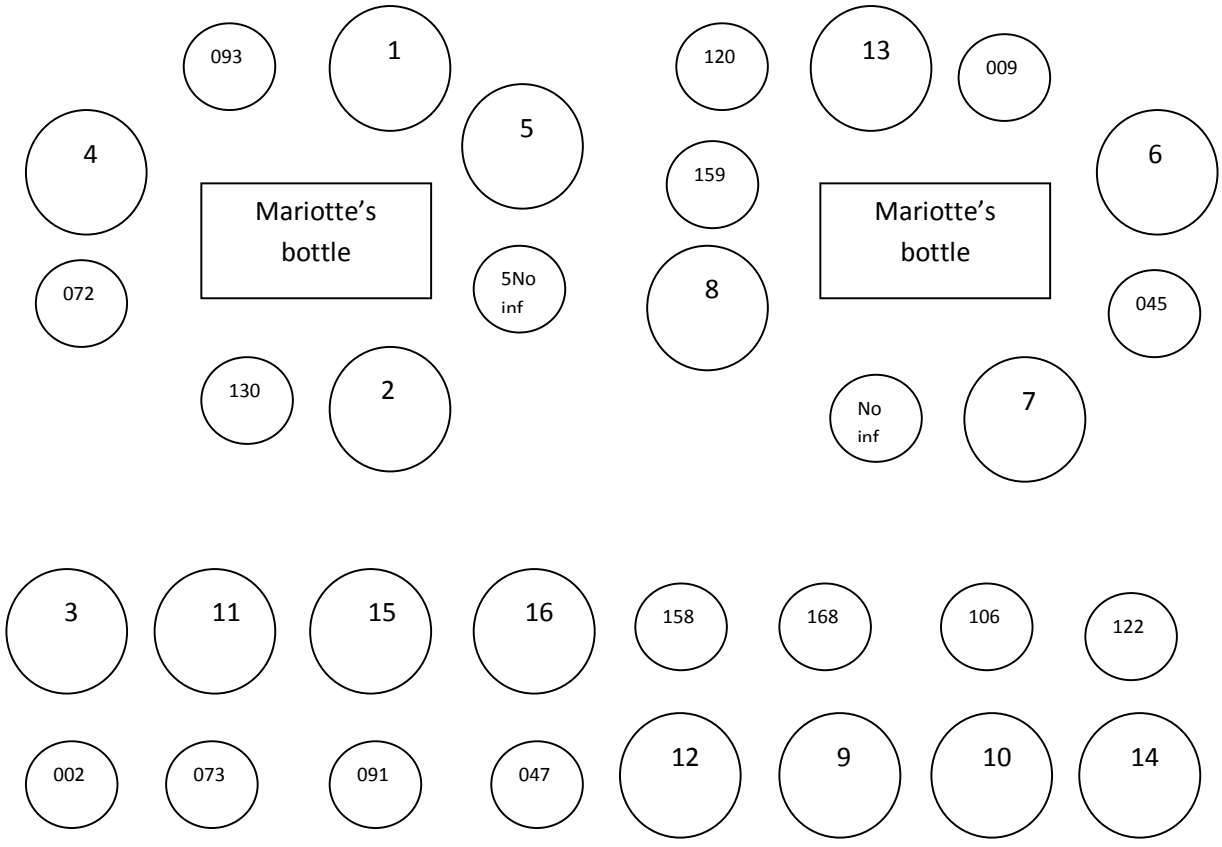

Figure 8. Field and lab experiment sampling map

Where:

Small circles with three digit numbers are representing the small ring (inner diameter d_i=5.0cm), volume of 100cm³.

Bigger circles with one to two digits are the big rings (d_i=8.0cm), volume of 251cm³.

The inside numbers of circles are the actual ring numbers.

No inf – means no infiltration took place.

Readings of the cumulative infiltration were made manually every 2 min for at least 90 minutes or until the infiltration rates of three successive time intervals were constant.

The time allowed for infiltration at each replicate was set approximately 90 min. Also it was verified experimentally. Figure 9 gives an overview of the set up of the field experiment.

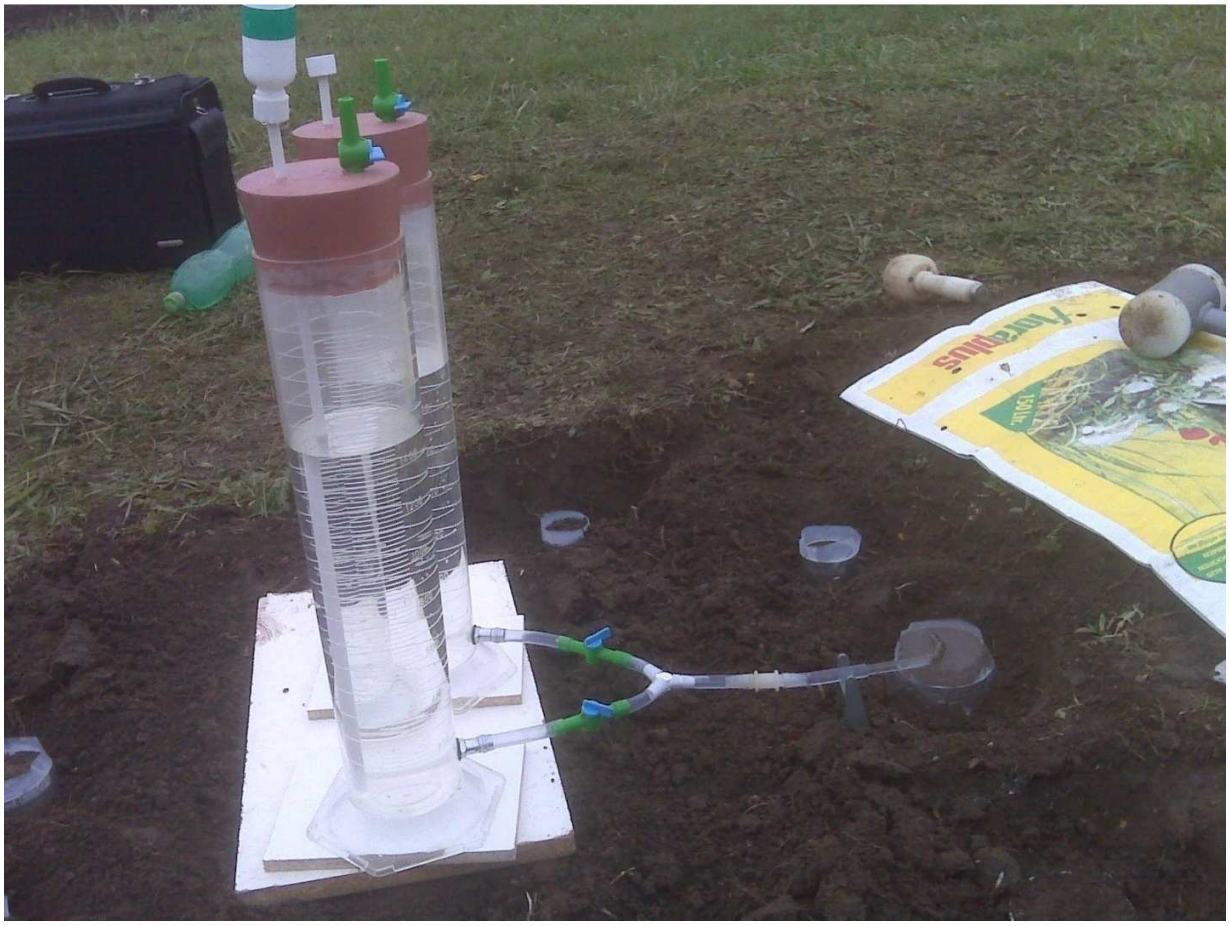

Figure 9. Experimental set up of a field measurement

As shown in Figure 9 and Figure 10 to maintain the constant water head on the ring surface, the plastic sticky tape (2.0cm height) was used. In this purpose, the soil around the sampling ring was dug out and outer wall of the ring became ready to be extended by plastic tape (Figure 10).

Figure 10. Constant water head maintained by plastic tape.

Normal tap water was used for the experiments. The same experimental procedure was applied on 2 sets of soil core samples. Both two sets had 4 big and 4 small replicate undisturbed soil core samples.

After the field K_s measurement, each core was taken to the lab, then it was saturated from the bottom on filter paper and the saturated hydraulic conductivity K_s, was measured in the lab.

No infiltration (zero infiltration) took place in 24 hours with allowed ponded water head condition for one small ring sample (Appendix 6). Therefore one infiltration test of the small ring was missed from field experiment. It was small ring No. 005.

4.2 Laboratory experiments

For laboratory analysis 32 undisturbed soil samples, 16 samples from areas surrounding and each of the replicate rings(16) after field measurement, were taken to laboratory test. The measurements were conducted in the laboratory, at the University of Life Sciences, Prague.

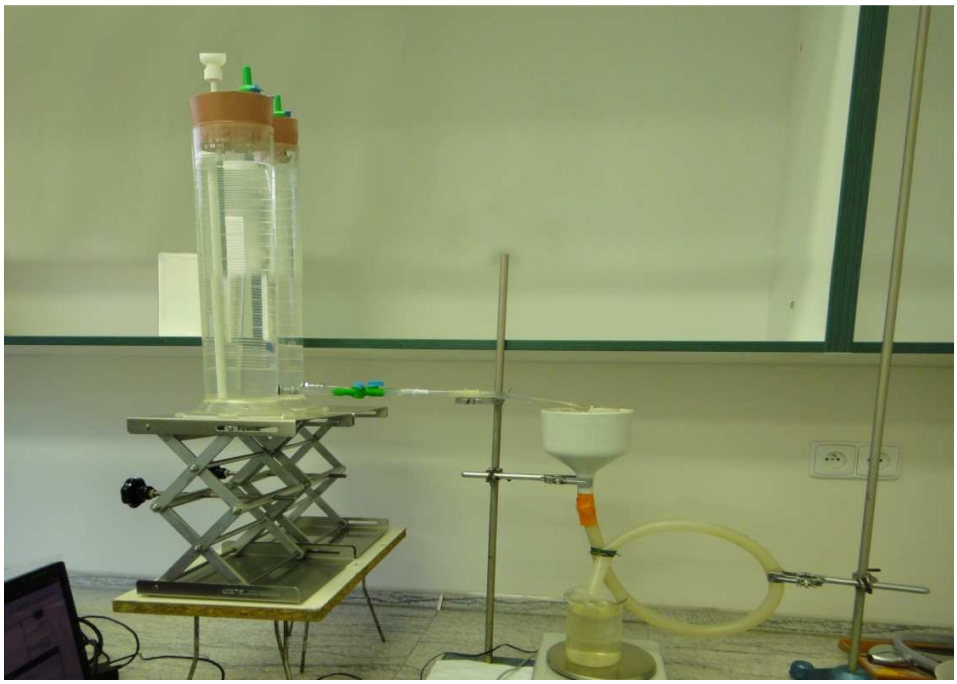

Figure 11. Lab experiment set up

The same constant head infiltrometer (Figure 11) used for laboratory analysis in addition digital data logging software (Figure 12) Dasy Lab (technical balance connected to Dasy Lab software) used to record data in the lab. Dasy Lab program uses an USB-based analog and digital input/output module USB-1208LS (Measurement Computing).

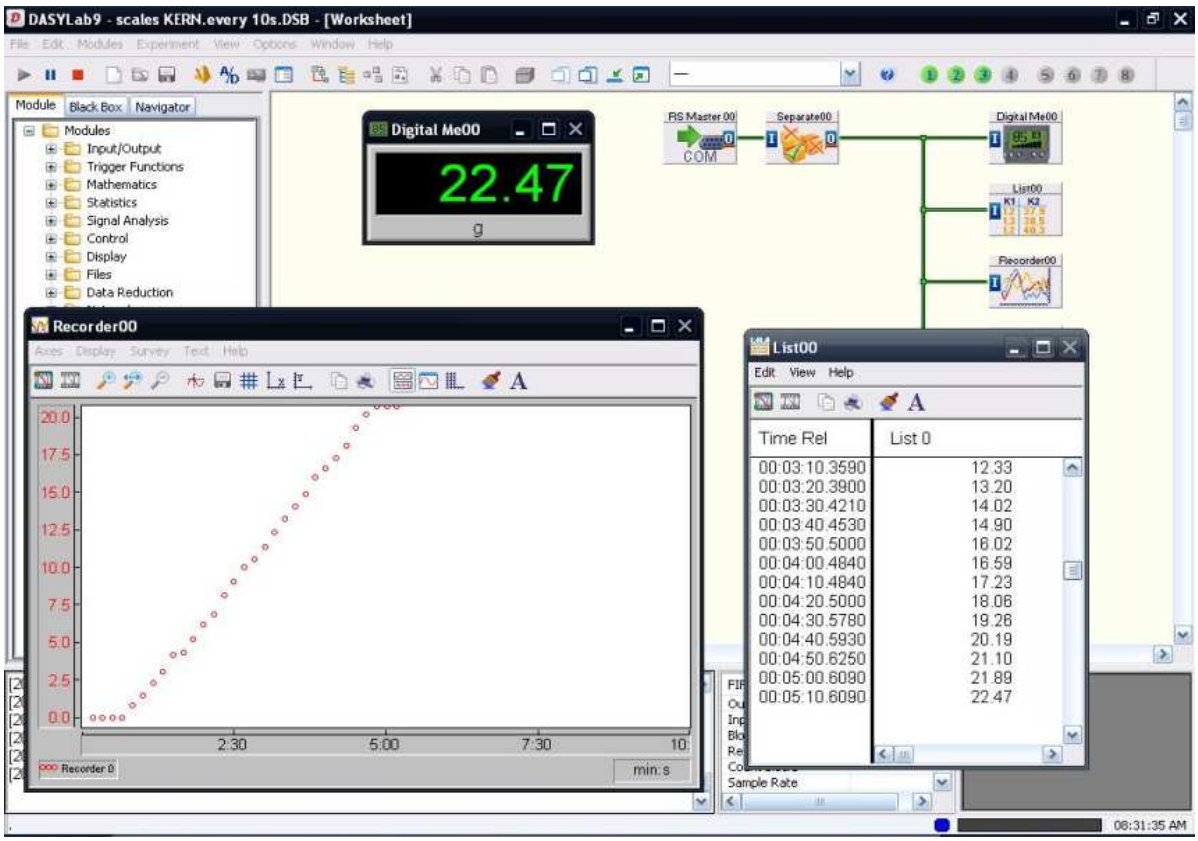

Figure 12. Dasy Lab reading

The samples were weighed and left to saturate on wet filter paper immersed in water. Finally, the cores were oven dried for 24 hours at 105°C and then measured the mass of dry soil sample. Initial and final volumetric moisture content as well as moisture content at saturation, dry bulk density, particle density and porosity were determined and calculated.

During particle density determination procedure some relatively big stones (Figure 13) found in few replicates. And the stone effect is remarkable for this relatively small size of core samples. It influences the dry bulk density, particle density and K_s measurement as well.

Figure 13. Stones in replicate.(big ring No. 12)

Also small ants did tremendous influence on infiltration test. The ants were found in few samples and they made many unusual holes. Four samples (small ring No. 093 and 072 or big ring No. 5 and 7) were significantly affected and their K_s were increased dramatically, because of ant-made preferential flow ways.

5 RESULTS

Based on field experiment manual reading (Appendix 7) from Mariotte' bottle, infiltration rate and cumulative infiltration graphs are drawn at each replicate and shown one of the example in Figure 14 and Figure 15.

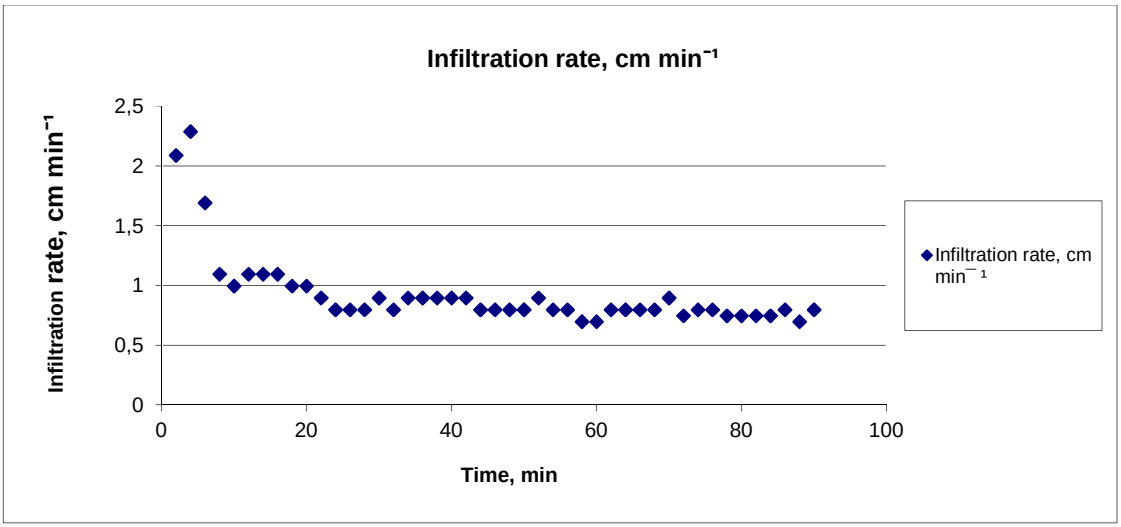

Figure 14. Field experiment Infiltration rate graph (example: big ring No.6)

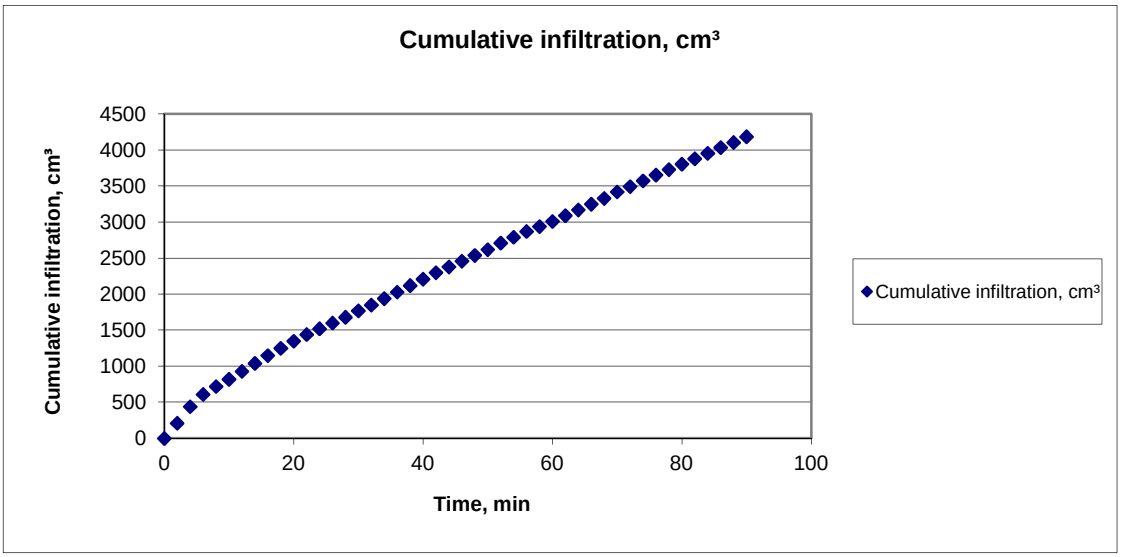

Figure 15. Field experiment Cumulative infiltration graph (example: big ring No. 6)

Then saturated hydraulic conductivity was calculated for each sampling ring. An example of calculation shown in Table 2.

Table 2. K_s calculation based on field experiment data. (example: big ring No. 6)

		Calculation
	Q , $cm^3\ min^{-1}$	40.07
	L, cm	5.00
	h, cm	1.50
	r, cm	4.00
	ΔH, cm	6.50
$K_S=(Q*L)/(\pi*r^2*\Delta H)$	K_s , $cm\ min^{-1}$	0.61
	K_s, $m\ s^{-1}$	1.02E-04

It shows K_s at $cm\ min^{-1}$ and $m\ s^{-1}$ units. But further analysis only unit of $cm\ min^{-1}$ was taken into account. The field experiment results are summarized in Table 3. The average K_s of big ring is $0.62cm\ min^{-1}$ while small ring K_s average is $0.35\ cm\ min^{-1}$.

Table 3. Summary of field experiment

Replicate	Infiltration rate, i, $cm\ min^{-1}$	Infiltration rate, i, $cm^3\ min^{-1}$	Constant head, h, cm	K_s, $cm\ min^{-1}$	Ring No.	Set No.	Ring type
1	0.90	46.48	1.5	0.71	2	1	big
3	0.99	50.22	1.5	0.77	4	1	big
6	0.40	20.44	1.3	0.32	1	1	big
7	0.80	40.23	1.4	0.63	5	1	big
9	1.20	60.60	1.6	0.91	7	2	big
10	0.60	27.61	1.4	0.43	8	2	big
11	0.75	38.46	1.5	0.59	13	2	big
14	0.80	40.07	1.5	0.61	6	2	big
2	0.89	18.37	1.5	0.72	130	1	small
4	0.60	11.74	1.3	0.48	72	1	small
5	0.64	12.62	1.3	0.51	93	1	small
12	0.25	4.94	1.5	0.19	9	2	small
13	0.25	4.79	1.5	0.19	120	2	small
15	0.20	3.70	1.5	0.15	45	2	small
8	0.25	5.00	1.5	0.20	159	2	small
			K_s average of big ring	0.62			
			K_s average of small ring	0.35			

Figure 16 and Figure 17 show bar charts of field experiment K_s. Sampling ring number and different sizes are marked.

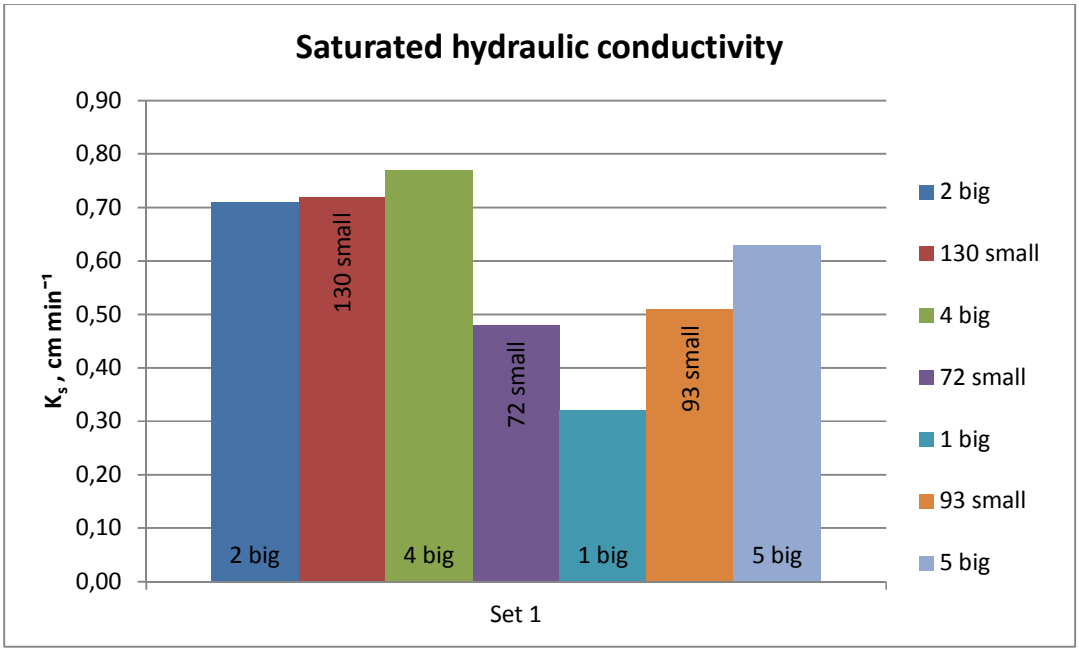

Figure 16. Set 1 K_s graph

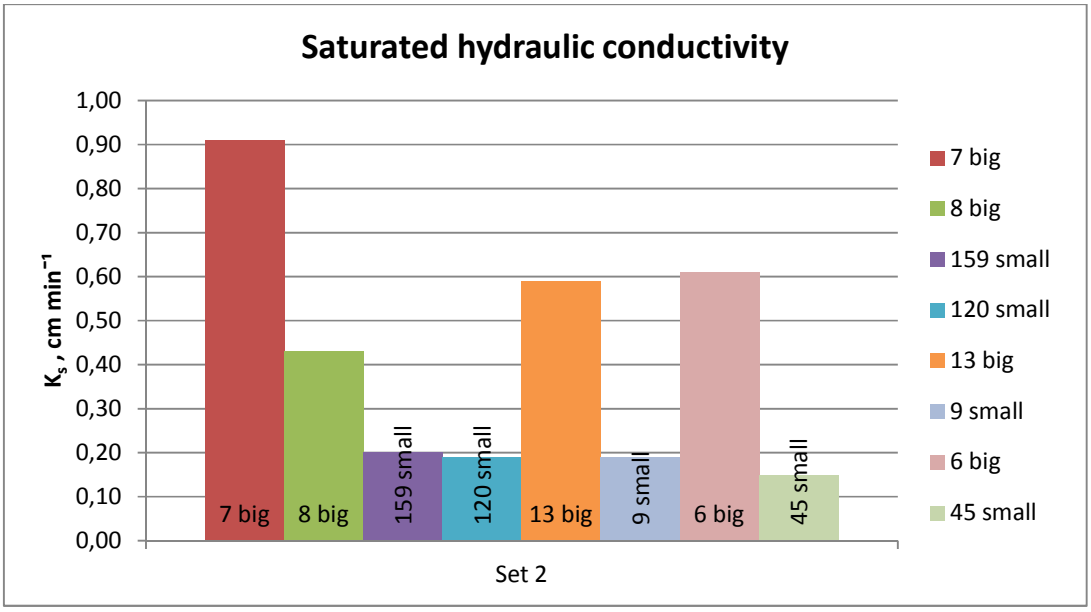

Figure 17. Set 2 K_s graph

Lab experiment data was automatically collected on Dasy Lab supported by ASC format. Data series with ASC format reading can be easily converted to MS Excel worksheet. And manual readings from Mariotte's bottle pasted in the right cell column of the sheet to make the readings easy to compare (Table 4). Reading of the Dasy Lab is included the beaker tare weight. Two sizes of beaker with tare weight of 139.3g and 99.8g were used.

Table 4. Laboratory experiment data logging (example small ring No. 122)

Lab experiment- Ring No. 122 Small ring
Reading: every 2min Technical balance (Dasy Lab)
Recording Date 06.12.2011, 08:00:00 AM

	Dasy Lab reading			Mariotte's bottle reading		
Time, min	**Reading, g**	**Infiltration, g**	**Cumulative infiltration, g**	**Reading, cm³**	**Infiltration, cm³**	**Cumulative infiltration, cm³**
00:00,0	0	0.00	0.00	2000	0	0.00
02:00,0	221.20	81.90	81.90	1940.00	60.00	60.00
04:00,0	173.66	73.86	155.76	1870.00	70.00	130.00
06:00,0	220.41	81.11	236.87	1780.00	90.00	220.00
08:00,0	176.08	76.28	313.15	1700.00	80.00	300.00
10:00,0	217.86	78.56	391.71	1620.00	80.00	380.00
12:00,0	184.89	85.09	476.80	1540.00	80.00	460.00
14:00,0	217.60	78.30	555.10	1480.00	60.00	520.00
16:00,0	180.40	80.60	635.70	1400.00	80.00	600.00
18:00,0	213.69	74.39	710.09	1320.00	80.00	680.00
20:00,0	179.84	80.04	790.13	1240.00	80.00	760.00
22:00,0	213.38	74.08	864.21	1160.00	80.00	840.00
24:00,0	181.33	81.53	945.74	1080.00	80.00	920.00
26:00,0	214.02	74.72	1020.46	1000.00	80.00	1000.00
28:00,0	180.60	80.80	1101.26	920.00	80.00	1080.00
30:00,0	213.72	74.42	1175.68	840.00	80.00	1160.00

Cumulative infiltration graph (Figure 18) of Dasy Lab reading and Mariotte's bottle reading done simultaneously. Then saturated hydraulic conductivity calculated (Table 5) based on Dasy Lab and Mariotte's bottle reading.

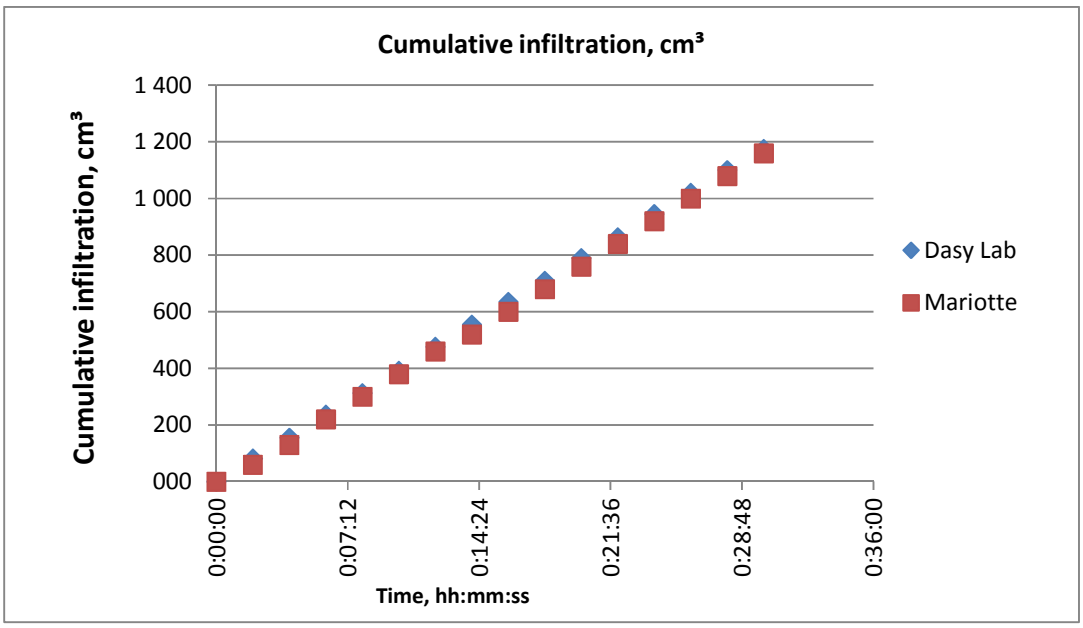

Figure 18. Lab experiment cumulative infiltration graph (example small ring No. 122)

Table 5. Lab experiment K_s calculation (example small ring No. 122)

		Dasy Lab	Mariotte's bottle
	Q , $cm^3\ min^{-1}$	39.62	39.23
	L, cm	5.10	5.10
	h, cm	1.40	1.40
	r, cm	2.50	2.50
	ΔH, cm	6.50	6.50
$K_s=(Q*L)/(\pi*r^2*\Delta H)$	K_s, $cm\ min^{-1}$	1.58	1.57

In this example automatic reading of Dasy Lab is slightly bigger than Mariotte's bottle manual reading. Therefore two reading series square difference and Root mean square difference (RMSD) were analyzed in Table 6. In total eleven measurements done simultaneously on Dasy Lab and Mariotte's bottle system. Five Dasy Lab measurements average were higher than Mariotte's bottle reading. Four Mariotte's bottle readings were higher than Dasy Lab. Two reading were equal to each other. And RMSD is 0.08cm min^{-1}. The assumption was not confirmed by statistical analysis. From statistical point of view for Dasy Lab reading and Mariotte's bottle reading there was no evidence to use correction factor.

Table 6. RMSD calculation of two reading series.

	K_s cm min^{-1}		
Ring number	Dasy Lab	Mariotte's bottle	Square difference
10 big	0.13	0.13	0.00
14 big	0.43	0.42	0.00
15 big	2.25	2.36	0.01
16 big	0.96	0.98	0.00
11 big	0.08	0.07	0.00
122 small	1.58	1.57	0.00
047 small	1.27	1.22	0.00
158 small	1.68	1.77	0.01
159 small	0.39	0.39	0.00
093 small	6.01	6.18	0.03
120 small	0.77	0.65	0.01
	SSD		0.07
	RMSD		0.08

If show Dasy Lab and Mariotte's bottle reading differences (Figure 19).

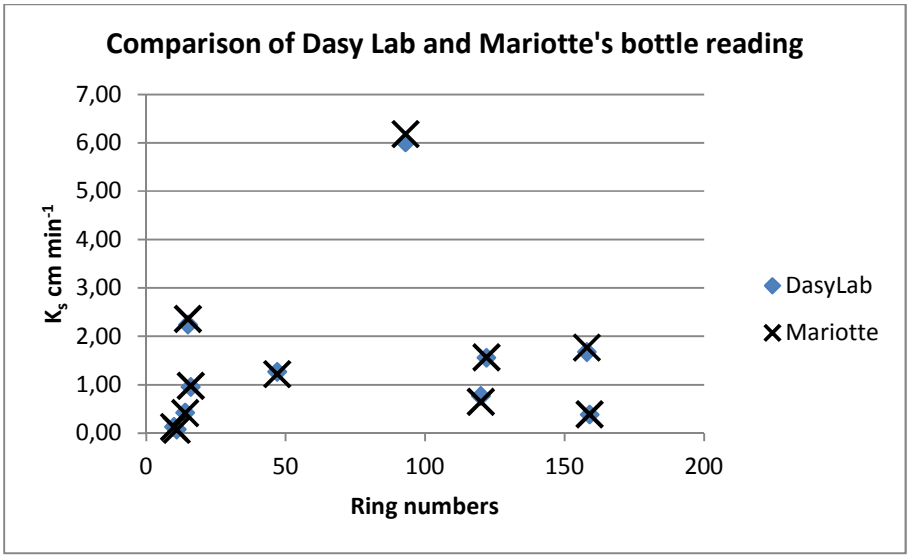

Figure 19. Comparison of Dasy Lab and Mariotte's bottle reading

The lab and field experiment infiltration rate [cm^3 min^{-1}], K_s [cm min^{-1}], dry bulk density [g cm^{-3}] of individual rings, some particle density [g cm^{-3}] measurement result is summarized in Table 7.

Table 7. Summary of all experiment

Ring No.	Infiltration rate, i, $cm^3\ min^{-1}$		K_s, $cm\ min^{-1}$		Dry Bulk density	Particle density	Ring type
	Field	Lab	Field	Lab	$g\ cm^{-3}$	$g\ cm^{-3}$	
2	46.48	56.38	0.71	0.86	1.29		big
4	50.22	6.10	0.77	0.09	1.28	2.65	big
1	20.44	123.71	0.32	1.89	1.35		big
5	40.23	81.48	0.63	1.25	1.34		big
7	60.60	52.27	0.91	0.80	1.26	2.62	big
8	27.61	56.32	0.43	0.86	1.34		big
13	38.46	143.00	0.59	2.14	1.34		big
6	40.07	8.30	0.61	0.13	1.41		big
3		1.51		0.02	1.62	2.63	big
9		8.94		0.14	1.44		big
10		8.81		0.13	1.46		big
12		2.30		0.04	1.52	2.63	big
14		27.83		0.43	1.43		big
15		146.70		2.25	1.5	2.62	big
16		63.47		0.96	1.31		big
11		5.10		0.08	1.46		big
130	18.37	36.69	0.72	1.42	1.26		small
072	11.74	73.24	0.48	2.88	1.35		small
093	12.62	152.71	0.51	6.00	1.08	2.62	small
009	4.94	0.50	0.19	0.02	1.44		small
120	4.79	19.73	0.19	0.77	1.36		small
045	3.7	0.14	0.15	0.01	1.46		small
159	5.00	9.83	0.20	0.39	1.29		small
122		39.23		1.58	1.35		small
047		31.79		1.27	1.46		small
168		3.03		0.12	1.42		small
091		1.34		0.05	1.42		small
106		0.67		0.03	1.62		small
002		0.67		0.03	1.5	2.63	small
073		0.67		0.03	1.46		small
158		42.74		1.68	1.14	2.64	small
005		0.13		0.00	1.46	2.62	small
	Average of big ring		0.62	0.75	1.40	2.63	
	Average of small ring		0.35	1.02	1.38	2.63	

The initial and saturated soil moisture content, dry bulk density, particle density, porosity for all rings are summarized in Table 8.

Table 8. Summary of initial and saturated physical properties for soil samples.

Ring type	Number of replicates	θ Initial mean	θ Saturated mean	Bulk density mean, g cm^{-3}	Particle density mean, g cm^{-3}	Porosity, %
All rings	32	0.21	0.28	1.39	2.63	47.23
Small rings	16	0.21	0.28	1.38	2.63	47.54
Big rings	16	0.21	0.30	1.39	2.63	47.12

Figure 20 shows overview of K_s measurement including field and lab experiment. From this figure one of the big outlier (small ring No. 093) was clearly seen.

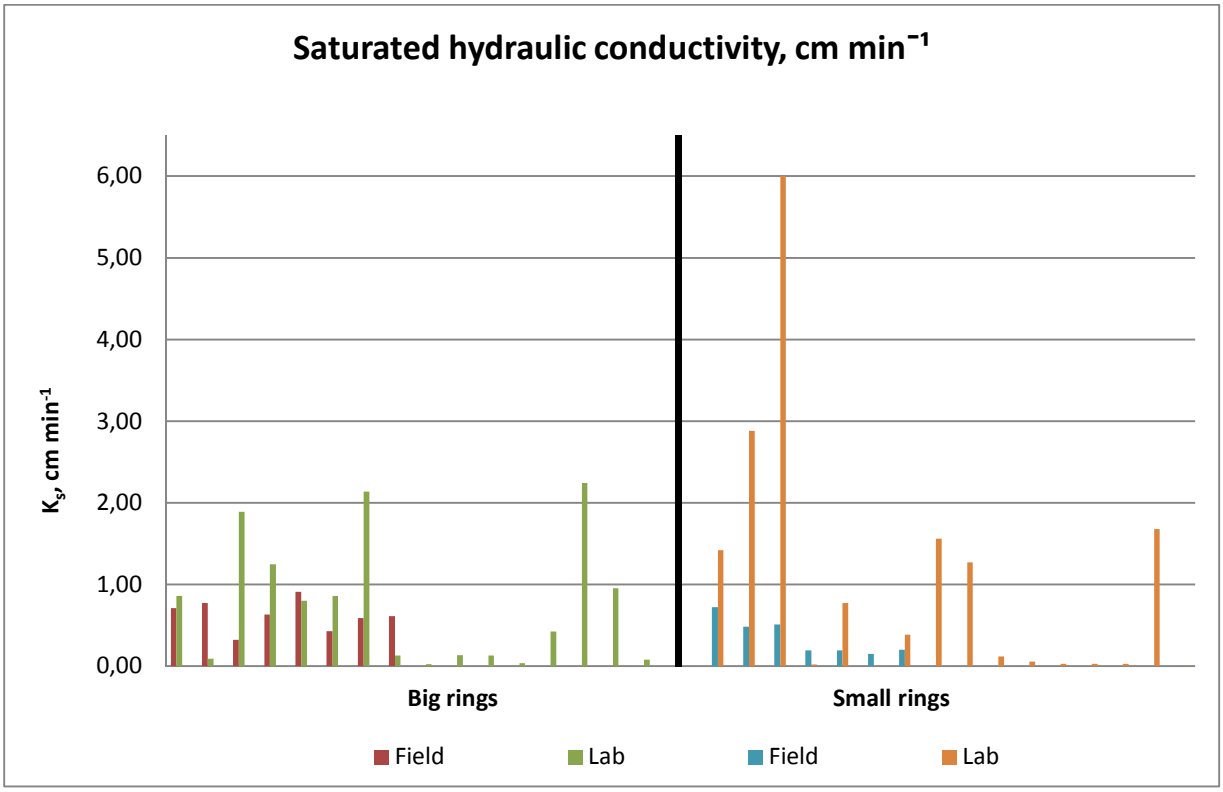

Figure 20. Field and Lab experiment comparison on differently sized core samples

The ring No. 093 is mostly affected by ant-made holes and preferential flow dominated which was obvious that is not occurred naturally. Thus this ring result was removed from further statistical analysis.

Soil physical properties and saturated hydraulic conductivity are shown on a graph (Figure 21) to investigate there is any relationship between dry bulk density or particle density and K_s.

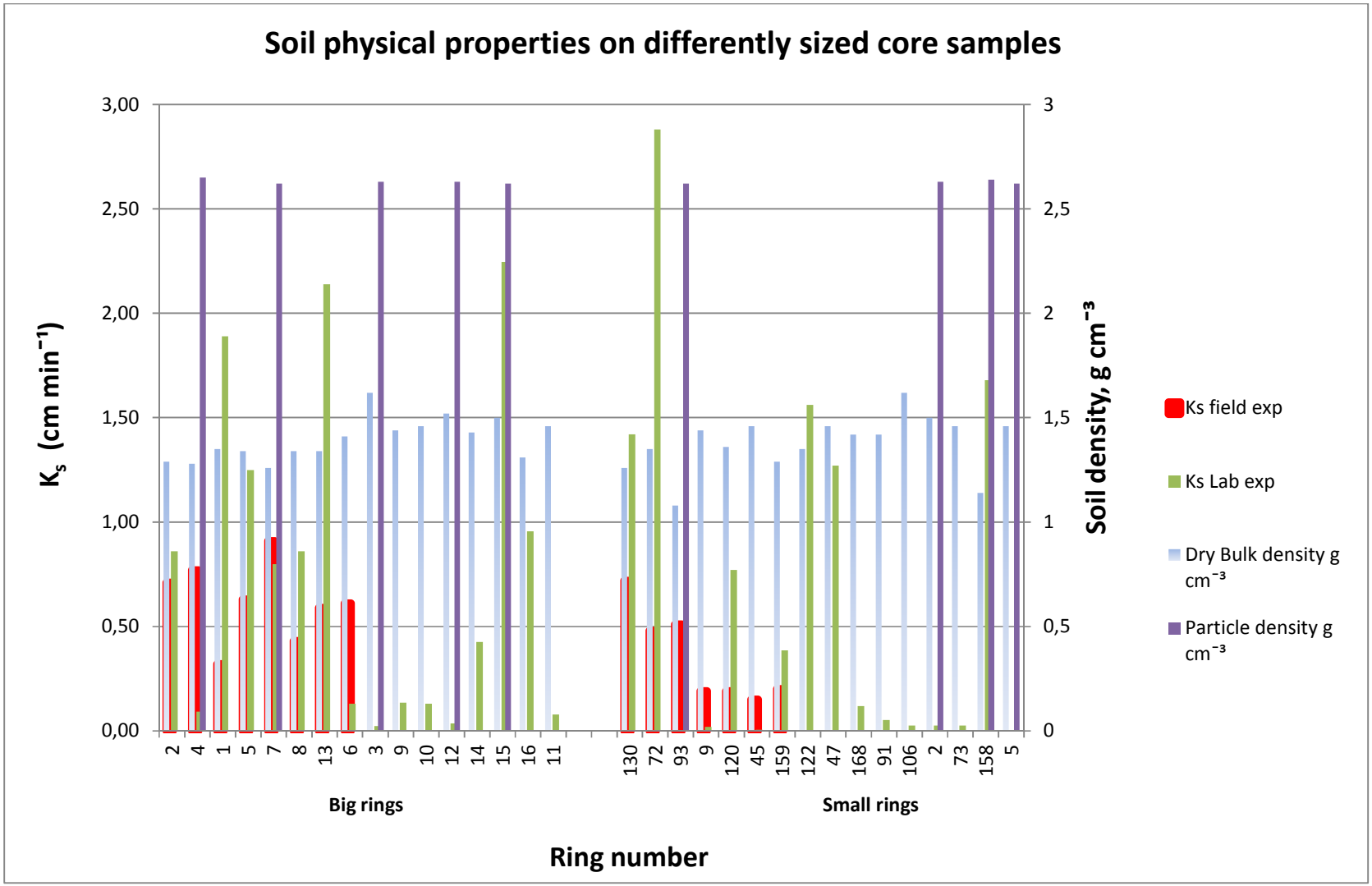

Figure 21. Soil physical properties on differently sized soil core samples

Statistical analysis

An analysis of variance ANOVA ($\alpha = 0.05$) for the data calculated by MS Excel. To determine whether there were significant differences in saturated hydraulic conductivities measured for different core sample ring size. Also an interaction between the field and lab measurement was considered.

If see the K_s average (Table 3) of small and big rings at field measurement it can say the bigger ring infiltrates through over two times larger soil area (50cm²) than the small ring (19.6cm²) and may therefore more macropores and other soil heterogeneities could happen. However porosity (Table 8) result presents there is no difference.

All series of data divided into four groups in order to do comparison: big ring from field experiment, small ring from field experiment, big ring from lab experiment and small ring from lab experiment. All statistical tests of the K_s values were therefore carried out using the 4 groups of data set in Table 9. Also, arithmetic means, standard deviation factors and coefficients of variation were calculated.

Table 9. Comparison of main statistical parameters for K_s

	Saturated hydraulic conductivity K_s, cm min^{-1}			
Parameters	**Big ring field**	**Small ring field**	**Big ring Lab**	**Small ring Lab**
STD	0.185890713	0.221014975	0.772707893	0.884117416
Variance	0.034555357	0.048847619	0.597077488	0.781663605
Median	0.62	0.20	0.61	0.12
Mean	0.62	0.35	0.75	0.68
Min	0.32	0.15	0.02	0.00
Max	0.91	0.72	2.25	2.88
Range	0.59	0.57	2.22	2.88
Mode	NA	0.19	0.86	NA

Statistical parameters graph is done using log-normal scale, which is common for this type of analysis. (Figure 22)

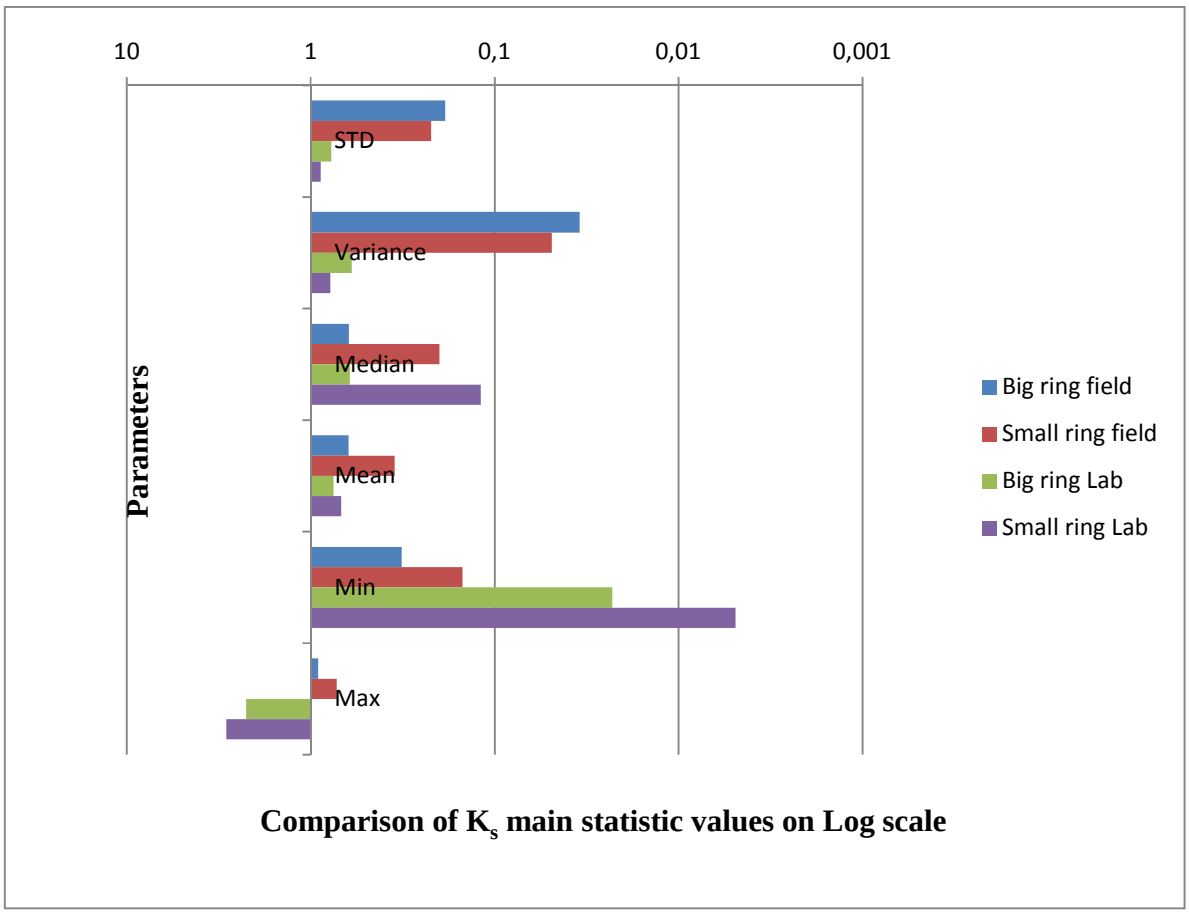

Figure 22. Comparison of K_s main statistic values on Log scale

To find out differences among the K_s measurements conducted in a field and laboratory or big and small core samples ANOVA statistical analysis done. And there was no significant difference between big or small and lab or field analysis at the statistical probability level α = 0.05 assumed. (Table 10)

Table 10. Analysis of variance done using four groups of data.

Anova: Single Factor

SUMMARY

Groups	*Count*	*Sum*	*Average*	*Variance*
Big ring field	8	4.97	0.62125	0.034555
Small ring field	7	2.44	0.348571	0.048848
Big ring Lab	16	12.0496	0.7531	0.597077
Small ring Lab	16	16.24528	1.01533	2.496446

ANOVA

Source of Variation	*SS*	*df*	*MS*	*F*	*P-value*	*F crit*
Between Groups	2.382778	3	0.794259	0.727625	0.541126	2.821628
Within Groups	46.93782	43	1.091577			
Total	49.3206	46				

F=0.727625 calculated is lower than Fcritical=2.821628 and P=0.54 value is higher than α=0.05. Null hypothesis is not rejected. There was an evidence to keep null hypothesis that means there was no significant difference between four groups average K_s. It yields Saturated hydraulic conductivity measured in the lab or field and core sample size big or small don't influence on average K_s. If exclude one big outlier ring No. 093, ANOVA result is shown in Table 11.

Table 11. Analysis of variance done excluding outlier small ring No. 093 result.

Anova: Single Factor

SUMMARY

Groups	*Count*	*Sum*	*Average*	*Variance*
Big ring field	8	4.97	0.62125	0.034555
Small ring field	7	2.44	0.348571	0.048848
Big ring Lab	16	12.0496	0.7531	0.597077
Small ring Lab	15	10.24528	0.683019	0.781664

ANOVA

Source of Variation	*SS*	*df*	*MS*	*F*	*P-value*	*F crit*
Between Groups	0.828226	3	0.276075	0.567433	0.639536	2.827049
Within Groups	20.43443	42	0.486534			

Total	21.26265	45

F calculated ratio including ring No. 093 is 0.727625. F calculated ratio excluding ring No. 093 is 0.567433.

While both cases F critical value is equal to 2.8, which is much higher than F calculated ratios. Based on this ANOVA result, ring No. 093 does not influence as much as shown on graph (Figure 20). But the reason was obvious (Appendix 4) and it was not naturally occured. Thus the outlier was not counted in further statistical analysis.

When consider the ANOVA factor is only ring size. In this purpose data divided into two groups as big ring and small ring the statistical analysis of variance presents in Table 12.

Table 12. Analysis of variance done using 2 groups of data.

Anova: Single Factor

SUMMARY

Groups	*Count*	*Sum*	*Average*	*Variance*
Big	24	17.0196	0.70915	0.403946
Small	22	12.68528	0.576604	0.560487

ANOVA

Source of Variation	*SS*	*df*	*MS*	*F*	*P-value*	*F crit*
Between Groups	0.201656	1	0.201656	0.421294	0.519666	4.061706
Within Groups	21.061	44	0.478659			
Total	21.26265	45				

Based on this ANOVA test it can be conclude there is no significant difference (at α=0.05) between two groups average K_s. It presents differently sized core samples (big and small rings) have no influence on measured K_s.

6 DISCUSSION

Saturated hydraulic conductivity K_s on differently sized core samples (small and big) obtained, by means determined in the field and lab experiments. In order to see a statistical point of view each data set characterized accordingly, derived by using four different groups, some basic statistics such as mean value, standard deviation were considered. In particular the ANOVA was done by MS excel function at α=0.05. Table 9 and Figure 22 summarize and compare statistics obtained for each data set. A log scale needs to be used to keep together 46 resulting varieties of magnitude orders in the same diagram (Mohanty et al., 1994).

Most of the affecting factors for saturated hydraulic conductivity mentioned in Literature review were observed and confirmed by results of this study except soil texture or salinity and acidity factors. Soil samples measured in a field or undisturbed samples taken in a lab were more or less representative of one layer soil profile. Small and big rings had similar height of 5cm and 5.1cm. Therefore soil texture difference or soil salinity and acidity factors might not be a case for this study.

One of the important factor which is not mentioned in Literature review is soil compaction. It should be considered this kind of study and even observed during the field experiments. Figure 8 shows there were two rings with no infiltration. One is from set 1, another is from set 2. Ponded water head was maintained at 1.5cm and allowed 24 hours. But no infiltration took place. No rock fragments were found down the spot (Appendix 6). This can be explained by soil compaction factor only. Wheel-traffic is the main source of soil compaction in agricultural fields (Mohanty, 1994). Soil compaction was reported as a cause of several negative results such as large pores destruction, which reduces saturated hydraulic conductivity, from the aspect of surface soil hydrology and agriculture; surface runoff increase, soil water storage decrease, yield decrease. (Hillel, 1998)

During sample preparation process for particle density measurement, bigger stones (size of 1.5cm x 2cm x 1cm dimension) found (Figure 13) in some replicates and later these were connected to lower K_s values (Table 7). Big ring No. 3 and 12 or small ring No. 2 had been affected by stone or rock fragment factor. The dry bulk density (Table 7) measurement was

confirmed this trend. Dry bulk densities of these rings ranged between 1.5g cm^{-3} and 1.62g cm^{-3}. While the calculated average dry bulk density was 1.39g cm^{-3}. For example: big ring No. 12 K_s was 0.04cm min^{-1} which is very low among the whole K_s measurements. As rock fragment content increases, the area available for water flow decreases, and overall water movement can become restricted (Baetens, 2007).

The values of K_s (Table 9) for big ring in the field ranged between 0.32cm min^{-1} and 0.91cm min^{-1}, for small ring in the field ranged between 0.15cm min^{-1} and 0.72cm min^{-1}. Based on the result it can be concluded big ring can have more pores for preferential flow. However the K_s values from lab experiment (Table 9) for big ring ranged from 0.02cm min^{-1} to 2.25cm min^{-1}, for small ring ranged between 0.00cm min^{-1} and 2.88cm min^{-1}. Here some unequal condition should be mentioned. The lab measurement performed a month later from field experiment and the samples kept in a refrigerator at +4°C - +6°C. The field experiment done within 5 days, the sample temperature ranged between -1°C -+5°C. While lab experiment temperature ranged +20°C - +24°C. The temperature difference is approximately 20°C. It is confirmed that temperature increases and K_s increases too. An increase in water temperature from 10°C to 25°C will be result in a 45% increase in K_s all other factors remaining constant (Reynolds et al., 2000).

Also the idea of air entrapment was observed. Minimum K_s value (Table 9) of lab experiment was 0.00cm min^{-1} which is lower than field experiment. Field minimum K_s was 0.15cm min^{-1}. Undisturbed samples from eight big rings and eight small rings were taken after field measurement gone through in those soil rings. Approximately one to five days after field measurement the ring samples were taken from same plots and transferred to the lab. It means sixteen rings measured twice. Firstly processed in a field and then in a lab. Before the second measurement some air might be entrapped in soil core samples. This was an agreement with Bouwer, (1978) that entrapped air can reduce the measured K_s by a factor of two or more.

The significant difference, calculated as K_s values obtained from mentioned four groups of data set. When comparing four groups of data ANOVA (Table 10) it was found that there was no significant difference.

From the above mentioned Table 9 and Figure 22 the following relation can be observed:

a) The comparison between standard deviations ranged from 0.19 to 0.22 for field measurement. For lab experiment ranged between 0.77-0.88. With respect to reliability of result the field direct measurement is preferred (Klute, 1986).

b) The variance among four groups identifies small rings have higher variance in both lab and field experiment data.

c) The small rings K_s median values are much lower than mean values compare to big rings. This phenomenon can be explained by core sample size as affecting factor. Sampling a small volume results in an extreme variation in the measured soil properties. (McBratney, 1998)

d) The K_s mean values for small rings were smaller in field and lab conditions. In particular K_s measured in a field for small rings were much lower than big rings. It agreed with Mohanty et al., (1994) supposed the lowest average K_s values, possibly because of smaller sample size, the presence or absence of open-ended macropores. In other hand bigger sample size has a greater probability for the presence of large macropores, resulting in higher K_s values.

e) The logarithmic scaling shows the small ring lab data produces a distribution less spread.

f) For the lab data set, on the contrary, the standard deviation remains high and lab data distribution more spread. However lab set had more replicates.

g) Statistically, the highest ranged data set was in lab experiments, range was 2.88 for small rings and 2.22 for big rings. While the field experiment statistical range was 0.57-0.59. It is another confirmation of the field experiment preference.

In addition, microbiological factor such as earthworms and ants increased the macropores of the soil through the time. For small ring No. 093 the ants made many holes and caused pipe flow of water and this ring removed from the statistical analysis. Also small ring No. 072, big ring No. 5 and 9 were affected by same factor.

Both small and big ring measurements, however, show standard deviation distributions without specific trend and more or less accumulated around low values. Concerning measurement, standard deviation versus mean values graphics, represented on the logarithmic scale, show, on the contrary, that the small ring is more sensitive to random measurement errors than the big rings.

In addition, the standard deviation of the measurement in the case of the lab experiment is characterized by an increasing drift which is almost absent for the field measurements.

7 CONCLUSIONS AND RECOMMENDATIONS

A new simple constant head infiltrometer was developed. Its design factors such as water reservoir diameter, bubbling rate and volume, capacity were tested. The design consists of two Mariotte's bottle type of water cylinder reservoirs each of the volume is 2000ml. Reading metric scale (sub-div. ml) 10ml. Soil physical properties and K_s measured at 46 replicates along two different core sample size were used.

Further the effectiveness of new equipment observed on K_s measurement and it was assessed by statistical analysis. For very small flow rates, the diameter of reservoir seemed too big. However, in sense of minimizing equipment error the reading period of time can be set longer. Reading fluctuations were compared with digital reading Dasy Lab. For small ring K_s measurement fluctuations were larger. It recommends when measure K_s only on small core ring volume of approximately 100cm³ better to chose a smaller diameter of cylinder reservoirs.

Soil physical properties as well as K_s on a differently sized soil core samples were proposed. Comparison of differently sized soil core samples was possible to describe the observed cumulative ponded infiltration pattern accurate, with only a small underestimation or overestimation of the cumulative infiltration.

K_s values obtained through these 2 core sample size agreed well with values found using the same technique although the boundary conditions under which this method normally may be applied were not met. It was possible to describe the observed cumulative infiltration using constant head infiltrometer K_s estimated on different core sample size data agreed with no significant influence. Largest differences in saturated hydraulic conductivity were observed between unusual cases such as ant-made holes and the soil compaction.

The first hypothesis which is the size of soil sampling ring has not significant influence on the measured saturated hydraulic conductivity in our soil was true.

The second hypothesis was not true. However lab experiment fluctuation was seemed quiet high from the graphs (Figure 20 and 21). But statistically there is no significant difference between the field and lab experiment.

8 REFERENCES

Angulo-Jaramillo, R., Vandervaere, et al., (2000) Field measurement of soil surface hydraulic properties by disc and ring infiltrometers. A review and recent developments, Soil and Tillage Research, 55, 1–29, 2000.

Arya, L.M., Farrel, D.A. and Blake, G.R. (1975). A field study of soil water depletion patterns in presence of growing soybean roots. Determination of hydraulic properties of the soil. Soil Science Society of America Journal, 45, 1023-1030.

Baetens, J. (2007) The effect of rock fragments on hydrophysical properties of a small watershed in north Chile.

Bagarello, V., Iovino, M. Tusa, G. (2000) Factors affecting measurement of the near saturated soil hydraulic conductivity. Soil Science Society of America Journal, 64: 1203-1210

Bouma, J. (1983) Use of soil survey data to select measurement techniques for hydraulic conductivity. Agricultural Water Management 6:177–190.

Bouwer, H (1978) Groundwater hydrology. McGraw-Hill, New York, ISBN 0070067155

Buchter, B., Hinz, C. and Fluhler, H. (1994). Sample-size for determination of coarse fragment content in a stony soil. Geoderma, 63, 265-275.

Cornelis, W.M., Ronsyn, J., et al., R. (2001). Evaluation of pedotransfer functions for predicting the soil moisture retention curve. Soil Science Society of America, 65, 638-648.

Dane, J.H., Topp, G.C. (Ed.) (2002) Methods of soil analysis; Part 4 – Physical methods, p. 1692 (selected chapters)

Dunn, G.H., and Philips, R.E. (1991). Macroporosity of a well-drained soil under no-till and conventional tillage. Soil Science Society of America Journal. 55:817-823.

Hillel, D. (1998) Environmental soil physics. Academic Press, New York, USA

Klute, A. (Ed.) (1986) Methods of soil analysis; Part 1 – Physical and mineralogical methods, No.9, 2nd edition, p. 1188 (selected chapters)

Kutilek, M. and Nielsen, D.R. (1994) Soil hydrology

Lee, D.H. (2005) Comparing the inverse parameter estimation approach with pedo-transfer function method for estimating soil hydraulic properties. Geosciences Journal, 9, 269-276.

Matula. S (2003) The influence of tillage treatments on water infiltration into soil profile. Plant Soil Environment, 49, 2003 (7): 298–306

Matula. S (2005) Soil hydrophysical and Microbiological Characteristics Changes Originate in Repeated Identical Top-soil treatment, Geophysical research vol. 7, 09988, 2005. European GeoSciences Union.

McBratney, A.B. (1998). Some considerations on methods for spatially aggregating and disaggregating soil information. Nutrient Cycling in Agroecosystems, 50, 51-62.

McKenzie, N., Coughlan, K. and Cresswell, H. (2002) Soil Physical Measurement and Interpretation for Land Evaluation. (CSIRO Publishing: Melbourne).

Merdun, H. (2010) Alternative Methods in the Development of Pedotransfer Functions for Soil Hydraulic Characteristics. Soil physics

Mohanty, B.P., Kanwar, R.S. and Everts, C.J. (1994) Comparison of saturated hydraulic conductivity measurement methods for a glacial-till soil. Soil Science Society of America Journal, vol. 58. no. 3

Oosterbaan, R.J. and Nijland, H.J. (1994). Chapter 12 in: H.P.Ritzema (Ed.), Drainage Principles and Applications. International Institute for Land Reclamation and Improvement (ILRI), Publication 16, second revised edition, 1994, Wageningen, The Netherlands

Philip, J.R. (1969). Theory of infiltration. Advanced Hydroscience. 5:215–296.

Reynods, W.D. and D.E. Elrick, (2002a). Constant head well permeameter (vadose zone). In: Dane, J. H. and Topp, G. C. (Ed). Methods of soil analysis. Part 4. Physical methods.SSSA Book Series 5, Soil Science Society of America, Madison, USA, 844-858.

Reynods, W.D. and D.E. Elrick, (2002b). Pressure infiltrometer. In: Dane, J. H. and Topp, G. C. (Ed). Methods of soil analysis. Part 4. Physical methods. SSSA Book Series 5, Soil Science Society of America, Madison, USA, 826-836.

Reynods, W.D. and D.E. Elrick, and Topp, G. C. (1983). A re-examination of the constant head well permeameter method for measuring saturated hydraulic conductivity above the water table. Soil Science, 136, 250-268.

Reynods, W.D. and D.E. Elrick,. and Youngs, E. G. (2002). Ring or cylinder infiltrometers (vadose zone). In: Dane, J. H. and Topp, G. C. (Ed). Methods of soil analysis. Part 4. Physical methods. SSSA Book Series 5, Soil Science Society of America, Madison, USA, 818-826.

Reynods, W.D. and D.E. Elrick,.Youngs, E. G, Booltink, H. W. G. and Bouma, J. (2002). Saturated and field-saturated water flow parameters-Laboratory methods. In: Dane, J. H. and Topp, G. C. (Ed). Methods of soil analysis. Part 4. Physical methods. SSSA Book Series 5, Soil Science Society of America, Madison, USA, 802-803.

Reynolds, W.D., B.T. Bowman, R.R. Brunke, C.F. Drury, and C.S. Tan. (2000). Comparison of tension infiltrometer, pressure infiltrometer, and soil core estimates of saturated hydraulic conductivity. Soil Science Society of America Journal. 64:478-484.

Reynods, W.D. and D.E. Elrick, (1990). Ponded infiltration from a single ring: Analysis of steady flow. Soil Science Society of American Journal. 54: 1233-1241.

Snehota, M., Sobotkova, M., Cislerova,M. (2008) Impact of the entrapped air on water flow and solute transport in heterogeneous soil experiment set-up. Journal of Hydrology and Hydromechanics, vol. 56, no. 4, p. 247-256.

Spongrova, K., Kechavarzi, C., Dresser, M., Matula, S., Godwin, R.J. (2009) Laboratory and field testing of an automated tension infiltrometer. Biosystems Engineering

Topp, G.C, Reynolds, W.D., and Green, R.E. (1992) Advances in measurement of soil physical properties: Bringing theory into practice

White, I., Sully, M.J., and Perroux, K.M (1992) Measurement of surface-soil hydraulic properties: Disk permeameters, tension infiltrometers and other techniques In (Topp, G.C, Reynolds, W.D and Green, R.E eds.) Advances in Measurement of Soil Physical Properties: Bringing Theory into Practice. Soil Science Society of America Inc., Madison, Wisconsin, USA.

Wosten, J.H., Pachepsky, Y.A., and Rawls, W.J. (2001). Pedotransfer functions: bridging the gap between available basic soil data and missing soil hydraulic characteristics. Journal of Hydrology, 251, 123-150.

Wu, L., Pan, L., Mitchell, J. and B. Sanden (1999). Measuring Saturated Hydraulic Conductivity using a Generalized Solution for Single-Ring Infiltrometers. Published in Soil Science Society of America Journal.63:788-792.

Wu, L., Pan, L., Robertson, M.J. and P.J. Shouse (1997). Numerical Evaluation of Ring-Infiltrometers under various Soil Conditions. In Soil Science, Vol. 162, No.11.

Wu, L. and L. Pan (1997). A Generalized Solution to Infiltration from Single-Ring Infiltrometers

http://echo2.epfl.ch/VICAIRE/mod_3/chapt_8/main.htm

http://en.wikipedia.org/wiki/Disc_permeameter

http://www.usyd.edu.au

www.webofknowledge.com

www.waterlog.info

http://hydropedologie.agrobiologie.cz

9 APPENDICES

Appendix 1. One of the big ring measurement in the field.

Appendix 2. Technical balance reading (connected to the Dasy Lab software)

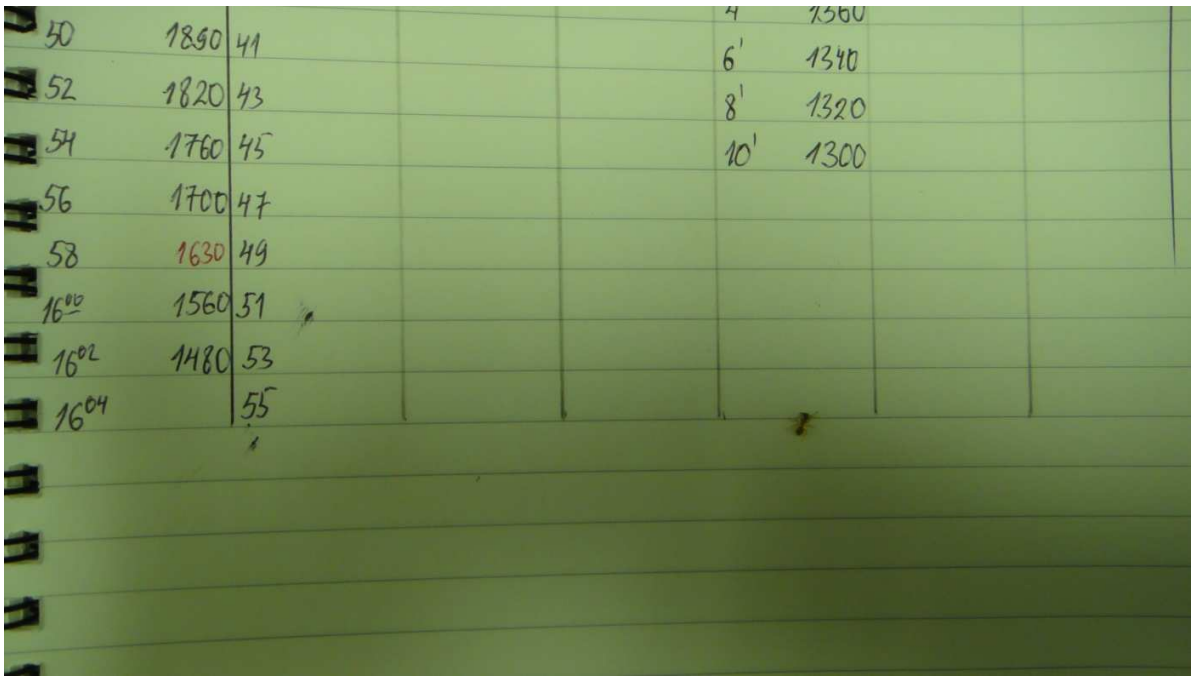

Appendix 3. Manual data logging and small ant is shown on the picture

Appendix 4. Example of ant-made holes and ants are up to the glass tube (Small ring No. 093)

Appendix 5. Stones found in some soil core samples. Example small ring No. 002.

Appendix 6. No infiltration spot(small ring No. 005). There were not rock fragments. Thus it was a soil compaction factor.

No	Time, min	Reading, cm^3	Infiltration, cm^3	Infiltration rate, cm min^{-1}	Cumulative infiltration, cm^3
1	0	2020	0		0
2	2	1810	210	2.09	210
3	4	1670	230	2.29	440
4	6	1560	170	1.69	610
5	8	1450	110	1.09	720
6	10	1350	100	0.99	820
7	12	1240	110	1.09	930
8	14	1130	110	1.09	1040
9	16	1020	110	1.09	1150
10	18	920	100	0.99	1250
11	20	820	100	0.99	1350
12	22	730	90	0.90	1440
13	24	650	80	0.80	1520
14	26	570	80	0.80	1600
15	28	490	80	0.80	1680
16	30	400	90	0.90	1770
17	32	320	80	0.80	1850
18	34	230	90	0.90	1940
19	36	1930	90	0.90	2030
20	38	1840	90	0.90	2120
21	40	1750	90	0.90	2210
22	42	1660	90	0.90	2300
23	44	1580	80	0.80	2380
24	46	1500	80	0.80	2460
25	48	1420	80	0.80	2540
26	50	1340	80	0.80	2620
27	52	1250	90	0.90	2710
28	54	1170	80	0.80	2790
29	56	1090	80	0.80	2870
30	58	1020	70	0.70	2940
31	60	950	70	0.70	3010
32	62	870	80	0.80	3090
33	64	790	80	0.80	3170
34	66	710	80	0.80	3250
35	68	630	80	0.80	3330
36	70	540	90	0.90	3420
37	72	465	75	0.75	3495
38	74	385	80	0.80	3575
39	76	1980	80	0.80	3655
40	78	1905	75	0.75	3730
41	80	1830	75	0.75	3805
42	82	1755	75	0.75	3880
43	84	1680	75	0.75	3955
44	86	1600	80	0.80	4035
45	88	1530	70	0.70	4105
46	90	1450	80	0.80	4185

Appendix 7. Field measurement data logging (manual reading of big ring No.